Deciphering the functional redundancy of USP4 and USP15

by

Sarah Zachariah

A thesis submitted in partial fulfillment of the requirements for the
Master of Science degree in Biochemistry

Department of Biochemistry, Microbiology, Immunology
Faculty of Medicine
University of Ottawa

Supervisor: Dr. Douglas Gray

ABSTRACT

The deubiquitinating enzymes USP4 and USP15 are encoded by genes that are ohnologues arising from whole genome duplication events early in vertebrate evolution, and the majority of known vertebrate genomes contain a functional copy of both. Both USPs are known to be involved in some of the same signalling pathways such as Wnt/β-catenin, however subfunctionalization has occurred such that they each regulate the stability of distinct substrates. Despite their sequence and evolutionary similarities, the ohnologues may have opposite correlations in overall survival of lung adenocarcinoma patients. Early work with knockout mice has determined that while mice null in one ohnologue display no phenotype, the double null genotype is lethal. We hypothesize that there are mechanisms in place that allow one to perform the other's functions to a certain extent when deficient in one USP. To study the extent of this functional redundancy, we are analyzing the progeny of genetic crosses of mice in which one or both genes have been inactivated. There is evidence for partial functional redundancy and more severe phenotypes when deficient in USP15. Embryos null for both genes die at midgestation and are physically smaller than embryos heterozygous for both genes. They have underdeveloped livers, and a likely defect in hematopoiesis. Proper fetal hematopoiesis requires signalling through Wnt/ β-catenin pathway, and a systematic analysis of the components of this pathway has been undertaken to correlate deficiencies with the genotypes of our knockout mice. There also may be preliminary evidence of transcriptional compensation in one ohnologue USP when the related USP is knocked out. These findings will have implications for potential targeted therapies.

ACKNOWLEDGEMENTS

I would first like to thank my supervisor, Dr. Doug Gray, for the opportunity to study in his lab over the last couple of years. His invaluable teaching and encouragement left me with lifelong skills and knowledge that I will apply to every aspect of my future career. Doug, thank you for always believing in me- I cannot imagine having done this research project without your support!

Second, I would like to thank the members of the Gray-Woulfe lab for their support and friendship throughout my degree. Josée has been an incredible mentor and my #1 cheerleader through it all. Thank you for patiently teaching me new skills and always being available to chat about results and life. Mei's expertise and support have been essential during my time in the lab. Kianna has been a great friend and mentor during my Master's and was always willing to provide me with guidance through the milestones.

I would like to also thank my thesis advisory committee members, Dr. Marc Ekker and Dr. Jonathan Lee for their advice and guidance. Thank you to the members of the third-floor cancer centre for making it a fun place to work. Finally, thank you especially to my family and friends for their incredible and continued support. Thank you for listening to me chat about USPs, encouraging me when I faced setbacks, and giving me the confidence to reach my goals.

TABLE OF CONTENTS

LIST OF ABBREVIATIONS

AGM	Aorta-gonad-mesonephros
APC	Adenomatous polyposis coli
CK1	Casein kinase 1
DMEM	Dulbecco's Modified Eagle Medium
DNA	Deoxyribonucleic acid
DUB	Deubiquitinating enzyme
DUSP	Domain in USP
Dvl	Dishevelled
EBI	Erythroblastic islands
EMT	Epithelial-mesenchymal transition
ES	Embryonic stem
Fz	Frizzled
GSK3β	Glycogen synthase kinase 3β
H & E	Hematoxylin and eosin
HSC	Hematopoietic stem cells
LGR5	Leucine-rich repeat-containing G-protein-coupled receptor 5
LRP5/6	Low-density lipoprotein receptor-related protein 5/6
MEF	Mouse embryo fibroblasts
(m)RNA	(messenger) Ribonucleic acid
NF-κB	Nuclear Factor kappa-light-chain-enhancer of activated B cells
NITC	Nonsense-induced transcriptional compensation
NSCLC	Non-small cell lung cancer
PBS	Phosphate-buffered saline
PCR	Polymerase chain reaction
PPIA	Peptidylprolyl Isomerase A
PVDF	Polyvinylidene fluoride
qPCR	Quantitative polymerase chain reaction
RT-PCR	Reverse transcription polymerase chain reaction
RQ	Relative quantification
Smad3/4	Mothers against decapentaplegic homolog 3
SSD	Small segmental duplication
TCF4	Transcription factor 4
TCF/LEF	T cell factor/lymphoid enhancer factor
TGF-β	Transforming growth factor beta
UBL	Ubiquitin-like domain
Unp	Ubiquitous nuclear protein
USP (4/15)	Ubiquitin-specific protease (4/15)
WGD	Whole genome duplication
Zeb1	Zinc finger E-box-binding homeobox 1
2R-WGD	Two rounds of whole genome duplication

Genotype Abbreviations:

Het/Het	Heterozygous for USP4, Heterozygous for USP15
Null/Null	Null for USP4, Null for USP15
Null/Het	Null for USP4, Heterozygous for USP15
Het/Null	Heterozygous for USP4, Null for USP15
Wt/Wt	Wildtype for USP4, Wildtype for USP15
Null/Wt	Null for USP4, Wildtype for USP15
Wt/Null	Wildtype for USP4, Null for USP4

LIST OF FIGURES

LIST OF TABLES

CHAPTER 1: INTRODUCTION

1.1 Ubiquitination

Ubiquitination is a reversible post-translational modification used by cells to control a wide variety of cellular processes. It involves the tightly controlled addition of a ubiquitin molecule, a 76-residue polypeptide, to a free amino group of a substrate protein. Ubiquitin itself has seven lysine residues, which can create a large variety of linkages, thus creating a variety of topologies. Ubiquitination is best known for its central role in the ubiquitin proteasome pathway, where it controls protein homeostasis. Proteolysis is most often triggered after a substrate's lysine residue is tagged with a polyubiquitin chain joined by lysine-48 (K-48) linkages, though other minor linkages are used as well (1). After a protein is ubiquitinated, it is sent to the 26S proteasome, through affinity of polyubiquitin chains for subunits of the 19S proteasome lid. The proteasome degrades the protein into small peptides and releases free ubiquitin molecules for re-use. Other linkages such as K63 act as modulators for protein-protein interactions and play a role in cell signaling (2). For example, this kind of ubiquitination is involved in scaffolding of signalling complexes, endocytic trafficking, DNA repair, cell cycle and apoptosis (3).

The addition of a ubiquitin molecule involves the coordination of E1 ubiquitin activating enzymes, E2 conjugating enzymes, and E3 ligases, which each use a catalytic cysteine residue sequentially to add ubiquitin to specific substrates (4). While there are a limited number of largely conserved E1 ubiquitin activating and E2 conjugating enzymes, hundreds of E3 ubiquitin ligases have evolved in response to the large variety of substrate proteins they must recognize (4). Ubiquitination is a dynamic process, therefore, as there are families of E3 ligases that catalyze the addition of ubiquitin, there are also families of proteins that catalyze the removal of ubiquitin.

1.2 Deubiquitinating enzymes and their evolution

The role of deubiquitinating enzymes (DUBs) is to cleave ubiquitin moieties from the free amino termini or internal lysine residues of substrate proteins. While E3 ligases promote degradation and protein instability, DUBs promote protein maintenance and stability. Much like the E3 ubiquitin ligases, there is a large variety of deubiquitinating enzymes. The DUB superfamily consists of 93 members, divided into six families based on sequence and domain conservation: ubiquitin carboxy-terminal hydrolases, ovarian tumour proteases, Machado-Josephin domain-containing proteases, motif-interacting with ubiquitin containing novel DUB family, JAB1 MPN MOV34 family, and finally, ubiquitin-specific proteases (USPs) (5). While the JAB1 MPN MOV34 family are zinc metallopeptidases, every other family are cysteine peptidases. The USP family has 56 members, making it the largest DUB family. Through its function of removing ubiquitin from substrate proteins, DUBs are involved in processes including transcription, DNA damage signalling, cell cycle progression, and more (5).

Of the members of the DUB superfamily, there is extensive functional redundancy in the many pathways they are involved in. Much of this functional redundancy is seen in paralogous DUB genes, meaning those that arose from a duplication event. Duplication events are considered to be the principal source of new genes (6). While these duplicated genes would initially have identical sequences, the few duplicates that are not silenced over time (by nonfunctionalization or pseudogenization) would eventually diverge. This divergence could allow for subfunctionalization, such as by the redistribution of substrates or by dividing gene expression such that the paralogues are expressed at different stages of development or in different cell types. Neofunctionalization, where novel functions are evolved, can also occur,

such as when the duplication temporally coincides with the appearance of a separate novel molecular pathway (7).

There are various factors that determine if a gene paralogue will be retained in the genome, but ultimately, it comes down to fitness. Natural selection will select for duplicated genes if they confer an increase in reproductive fitness. One model argues that new genes evolve under continuous selection. This model suggests that prior to duplication, the parent gene has a minor side function, in addition to its main function. When a new niche arises that favours this minor side function, selection will favour its amplification by increasing the gene's dosage. If a duplication event occurs, this selection pressure will allow an extra copy of this gene to be maintained and will favour the accumulation of mutations that improve the copy's ability to perform this side function. Over time, the new copy's function will no longer be a side function, but its full function (6).

There are a few forms of genetic duplication including retrotransposition, small segmental duplication (SSD), and whole genome duplication (WGD). Retrotransposition involves the transcription of genetic material into RNA, followed by reverse transcription back to DNA, and then insertion into the genome at specific sites. This method of gene duplication is particularly common in plants, and most repeat sequences in the human genome are derived from transposable elements (8). SSD can include anything from individual genes to short segments of genes that have been duplicated. Segmental duplications tend to be more common in humans than other organisms such as yeast or flies (8). WGD has only occurred twice in vertebrate evolution (with the exception of bony fishes), in what is referred to as the 2R-WGD hypothesis (9). It is hypothesized that these events occurred at the base of Vertebrata, the sub-phylum that we, along with jawless fish, jawed vertebrates, tetrapods, and bony fish, belong to. It is thought

that 2R-WGD is the reason for the increased complexity and size of the genome of vertebrates (10).

The 2R-WGD is largely responsible for the expansion of the DUB superfamily from 61 members in the ancestral vertebrate genome 500 million years ago, to the current 93 members that most metazoans have today (7). While most duplicated genes were silenced due to negative selection and genetic drift, those that were retained usually have high sequence similarity. These gene paralogues that arose from WGD and are retained in the genome are referred to as ohnologues, in recognition of Susumu Ohno who proposed the 2R-WGD hypothesis. Most DUB ohnologues have more than 50% sequence similarity, with a few exceptions such as USP18 and USP47, which only have 17% sequence similarity (7). As previously mentioned, some divergence had to occur in order to maintain these DUB ohnologues in the genome. Some of the ohnologue DUBs evolved spatiotemporal adaptations such as USP25 and USP28. USP25 has testis- and muscle-specific isoforms and USP28 has heart- and brain-specific isoforms (11). Other ohnologue DUBs appear to have divided up their respective substrates such as USP4 and USP15, where USP4 appears to have more substrates in innate immunity pathways and USP15 appears to have more substrates in TGFβ signalling (12). Finally, some evolved new functions such as USP16 and USP45. USP16 evolved a novel binding domain for HERC2 in its fifth exon, allowing it to participate in the downregulation of double stranded break repair, whereas USP45 is not involved in DNA damage response (13).

Ohnologues retain not only the coding sequence of the parent gene, but also the regulatory elements. This increases the potential for functional redundancy. Functional redundancy has not been well studied for most DUB ohnologues, therefore the Gray lab has been using the USP4/USP15 ohnologue pair as a system to study DUB evolution and functional redundancy.

1.3 Ubiquitin-specific protease 4 (USP4)

Ubiquitin-specific protease 4 (USP4) is a founding member of the USP family, the most abundant family in the DUB superfamily. USP4 was discovered in this lab during a survey of the genes near the Mpv 20 retroviral insertion site in 1993 (14). It was of particular interest since the predicted sequence was very similar to a human oncogene called tre-2 or TRE17. Since this was prior to the development of systematic nomenclature for the ubiquitin-specific protease family, this novel gene was called ubiquitous nuclear protein (*Unp*) due to a putative nuclear localization signal sequence similar to that in p53 (14). It was found also in the cytoplasm during cellular fractionation experiments by another group (15). Later, a nuclear export signal was found along with a nuclear import signal in the amino acid sequence of the protein which made it the first DUB to have nucleocytoplasmic shuttling abilities (16). The same group also found that the subcellular localization varied depending on cell type.

Usp4 (*Unp*, at the time) was found on mouse chromosome 9, and later mapped to the 3p21.3 region of the homologous human chromosome (17). This particular region was known to be frequently rearranged in human tumor cells. Indeed, when put under the control of a highly active promoter, high expression of *Usp4* resulted in the tumorigenic transformation of NIH3T3 cells when injected into athymic CD1 mice (17). The human homologue's mRNA was then found to be high in small cell tumors and adenocarcinoma of the lung. Recently, with the use of an online survival analysis software that uses human tumor transcriptomic data from multiple repositories, it can be seen that high expression of USP4 is correlated with decreased survival in lung adenocarcinoma patients (18) (Figure 1A). USP4 has also been associated with other cancers including liver (19) and breast (20).

The *Usp4* gene is comprised of 22 exons, yields a protein that is 963 amino acids and predicted to be 108.3 kDa. The mouse USP4 protein is 90% identical to the human homologue (17). The protein has two ubiquitin-like domains (UBL), a domain in USP (DUSP), two catalytic domains, and two linker domains. The first catalytic domain has the catalytic cysteine residue, encoded in exon 8, which gives the enzyme the 'cysteine protease' activity. The second catalytic domain has two histidine residues, encoded in exon 20, which makes up the catalytically-critical 'His box' (21). USP4 has the rare ability to efficiently cleave ubiquitin-proline bonds in synthetic test substrates (22); this property may relate to a flexible catalytic cleft that can accommodate unusual substrates, since ubiquitin-proline fusions do not occur naturally. In mammals, USP4 has two dominant isoforms, one including exon 7, and one skipping exon 7. This exon makes up the majority of a flexible linker region between the DUSP and a UBL, which form a critical interaction in the folding of the protein. A recent report from this lab suggested that the alternative splicing of USP4 in therian mammals is selectively maintained and that the two isoforms may target different cellular substrates in different compartments (23).

USP4 can cleave ubiquitin moieties from K48-linked ubiquitin chains, which are degradative, and K63-linked ubiquitin chains, which are regulatory (23). Over the years, USP4 has been found to be involved in an ever-growing list of cellular pathways necessary for cell fate, innate immunity, and development through the deubiquitination of substrates in the Wnt/ β-catenin (24), TGF- β (20), p53 (25), G protein-coupled receptor (26), and NF- κB pathways (27, 28). Additionally, USP4 has been found to interact with the spliceosome, thus is likely involved in RNA splicing (29). USP4 also has a number of proteins that it interacts with nonenzymatically. For example, USP4 has been seen to associate physically with the retinoblastoma gene product, pRb and pocket proteins p107 and p130 (30).

1.4 Ubiquitin-specific protease 15 (USP15)

Ubiquitin-specific protease 15 (USP15) was discovered a few years after USP4, at the same time that a systematic nomenclature for this family was proposed. The human *Usp15* gene is located on chromosome 12 at the 12q14 band, a different chromosomal location than *Usp4* (31). The *Usp15* gene encodes a protein of 952 amino acids and a predicted molecular mass of 109.2 kDa. The mouse USP15 protein is 98% identical to the human homologue (32). It is also a cysteine protease, meaning it has a catalytic cysteine residue and two histidine residues making up the "His box".

USP15 too has a role in cell growth, innate immunity and embryonic development, through interactions with Wnt/ β-catenin (33), TGF- β (34, 35), and NF- κB pathways (36). USP15 also interacts with the spliceosome (37). USP15 expression has been associated with glioblastoma, breast cancer, and ovarian cancer (35) . Interestingly, USP15 appears to have the opposite correlation with lung adenocarcinoma than USP4. Using the online survival analysis software that uses human tumor transcriptomic data from multiple repositories, it can be seen that high expression of USP15 is correlated with increased survival (18) (Figure 1B).

Upon its discovery, the human homologue of USP15 was known to be related to the human homologue of USP4 due to 56.9% sequence identity and 76% sequence similarity (31). They also share a common structural domain organization consisting of a DUSP (domain in USP) and two UBLs (ubiquitin-like) separated by a bi-part catalytic domain. USP15 also shares similar enzymatic activity to USP4, as it too can cleave ubiquitin from a synthetic peptide where a proline residue immediately follows the ubiquitin (32). This may be due to some flexibility in the catalytic domains, which may explain why these USPs are capable of cleaving ubiquitin chains of different topologies from a wide variety of substrates. As mentioned, USP4 and

USP15 appear to be functionally involved in many of the same cellular pathways including Wnt/β-catenin, TGF- β, NF- κB, and RNA splicing. These extensive similarities between the two USPs led to a phylogenetic study which found that USP4 and USP15 are ohnologues and arose from a whole genome duplication event in a jawed vertebrate ancestor during the Ordovician, approximately 500 million years ago (12). Interestingly, it appears that the ancestral USP was likely most similar to USP15.

However, if the majority of known vertebrate genomes, including human, contain a functional copy of both USP4 and USP15, they must have diverged sufficiently despite their partial functional redundancy and sequence similarity. In fact, they have. While they are involved in similar cellular processes, they have little overlap in terms of specific substrates. For example, both USPs upregulate the degradation of p53 by deubiquitinating, and thus, stabilizing E3 ubiquitin ligases that ubiquitinate p53 for downstream proteolysis. However, USP4 deubiquitinates ARFBP1 (25), while USP15 deubiquitinates MDM2 (38). In the TGF- β pathway, the type I TGF-β receptor is a substrate of both USP4 (20) and USP15 (35), however only USP15 also regulates some of the downstream effectors including Smad4 and APC (34, 35). Finally, USP4 has been demonstrated to associate with the proteasome (39), but USP15 has not. A full list of the known substrates of USP4 and/or USP15 was published in an article from this lab (Table 2 from source 37). Beyond the differences in substrates, there also may be evidence of spatiotemporal differences in expression between these two ohnologues. While both enzymes are ubiquitously expressed, USP15 has the highest levels of expression in oocytes, whereas USP4 has elevated expression throughout the immune system (40).

As both USP4 and USP15 are involved in a number of cancers, they have each been identified as targets for anticancer therapeutics, and in the case of USP4, an enzymatic inhibitor

has been identified (41). However, we recently argued that designing targeted therapeutics for ohnologue pairs such as USP4 and USP15 should be approached with caution due to potential functional redundancy and genetic compensation (42).

Figure 1. Kaplan-Meier plot of USP4/15 expression and lung adenocarcinoma overall survival. **(A)** High expression of USP4 (red) is correlated with lower overall survival in humans with lung adenocarcinoma compared to those with low expression of USP4 (black). **(B)** High expression of USP15 (red) is correlated with higher overall survival in humans with lung adenocarcinoma compared to those with low expression of USP15 (black). For both figures, data were accessed on kmplot.com, which is an online resource that uses gene chip and RNA-seq data from databases including Gene Expression Omnibus, The Cancer Genome Atlas, and European Genome-phenome Archive (18). The cut-off that defined "high" and "low" expression was arbitrarily set to the upper and lower 50%.

(A)

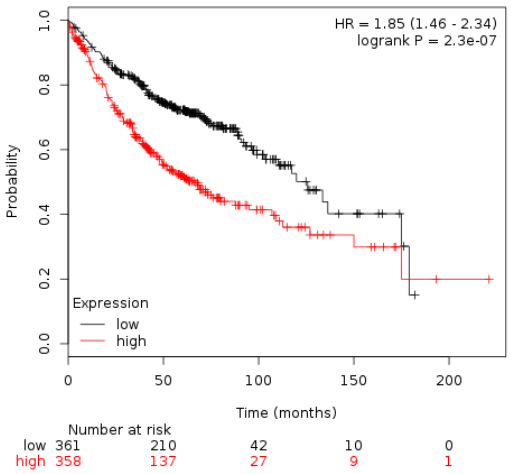
HR = 1.85 (1.46 - 2.34)
logrank P = 2.3e-07
Probability
Expression
low
high
Time (months)
Number at risk
low 361 210 42 10 0
high 358 137 27 9 1

(B)

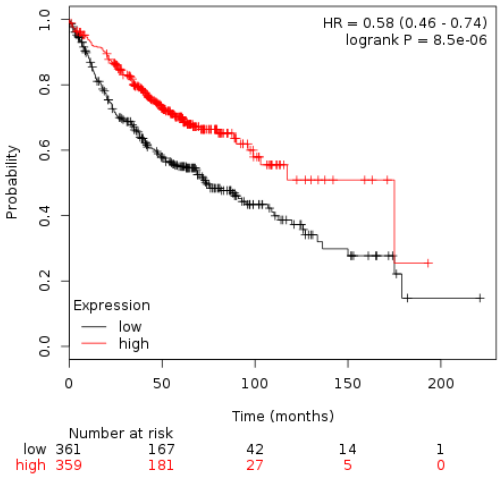
HR = 0.58 (0.46 - 0.74)
logrank P = 8.5e-06
Probability
Expression
low
high
Time (months)
Number at risk
low 361 167 42 14 1
high 359 181 27 5 0

1.5 Functional redundancy and genetic compensation

When an organism can maintain its viability and fitness despite genetic perturbations such as mutations, gene knockouts and knockdowns, it is said that this organism is genetically robust (43). This buffering system ensures that organisms will have similar outcomes in the face of minor genetic or environmental differences. We need not look far for evidence of such a system. An analysis of 589,306 human genomes found 13 healthy individuals with disease-causing mutations in 8 genes (44). The lack of any observable phenotype points to something causing this robustness. Natural selection has allowed the evolution of a number of different methods to acquire this genetic robustness. These methods include functional redundancy and genetic compensation.

Functional redundancy describes a situation where two or more genes have the same or overlapping functions, such that if one is inactivated, there is little to no observable phenotype (45). While there used to be a widespread view that genetic redundancy would be evolutionarily unstable, we now know that it is common and promotes stability. There are many examples of functional redundancy in our genome. For example, in the genes encoding actin-binding proteins, *ACTN2* and *ACTN3*, there is no phenotype when one is absent, despite them being differentially expressed spatially and temporally in mouse development (46). Much like USP4 and 15, *ACTN2* and *ACTN3* are ohnologues.

Genetic compensation is when levels of RNA or protein change to functionally compensate for the loss of function of another gene (43). Much like functional redundancy, there are a number of examples of genetic compensation. For example, in the absence of the ribosomal gene *Rpl22*, there are no translational defects due to a compensatory upregulation of *Rpl22l1* (47). Normally, RPL22 inhibits the expression of *Rpl22l1*, however in its absence this negative

feedback loop is no longer relevant and *Rpl22l1* is free to do the work of *Rpl22*. Interestingly, *Rpl22* and *Rpl22l1* are also ohnologues.

Related to genetic compensation is transcriptional adaptation, where related genes are upregulated without the use of protein feedback loops. Unlike the example of *Rpl22* and *Rpl22l1*, the mechanism of transcriptional adaptation is largely unknown. However, a recent Nature article by the Stainier group reported a requirement of transcriptional adaptation to be mutant mRNA degradation (48). Here, the authors describe a mechanism they coined "nonsense-induced transcriptional compensation (NITC)". As the name suggests, NITC requires nonsense-mediated mRNA decay, meaning that the mutant allele must still be transcribed to mRNA and it must contain a premature termination codon. When this mutant mRNA is transcribed and subsequently decayed, the fragments generated bind to the DNA sequences of highly related genes. This leads to transcriptional activation of these highly related genes to levels sufficient for rescue.

We recently published a paper in the journal *Bioessays: news and reviews in molecular, cellular and developmental biology*, in which we suggested that USP ohnologues would be good candidates for analysis for this mechanism (42). We did a systematic examination of the literature containing inactivating mutations in USPs in mice and found that in mice with homozygous knockout mutations in USP genes with a conserved ohnologue, the resultant phenotypes were mild to undetectable. In contrast, mice with knockout mutations in singleton genes (those without an ohnologue), the resultant phenotype was often lethal or dramatic. We suggested that this may be due to the NITC mechanism for genetic compensation proposed by the Stainier group (Figure 2).

As the Gray lab has been investigating the USP4/USP15 ohnologue pair, we have acquired mice with an inactivating mutation causing a premature stop codon in either USP4 or USP15. Genetic crosses of such mice have determined that while mice deficient in either USP4 or USP15 are viable, those deficient in both are not. This compound null genotype results in lethality with a high degree of confidence ($p = 0.000022$) (12). Therefore, this ohnologue pair is optimal to study a compensatory phenotype.

Figure 2. Compensation model for ohnologue DUBs. (A) Though 2R-WGD has initially given rise to several gene duplicates, many will be pseudogenized or lost over time (grey "inactive" gene), making them appear as singletons in our genome. Should a nonsense-inducing mutation occur, NITC would expect that nonsense-mediated decay will occur, producing transcript fragments. With no highly related ohnologue, we expect an observable phenotype to be produced. **(B)** Genes that arise from 2R-WGD and are not lost are often subfunctionalized, meaning the original gene's functions are divided amongst the ohnologues directly, or in a spatiotemporal manner (indicated by blue and red segments in the genes). Should a nonsense-inducng mutation occur, NITC would expect that nonsense-mediated decay will occur, producing transcript fragments that may induce the upregulation of the highly related and non-mutated ohnologue. This may mask the mutation and result in little to no phenotype. From Zachariah and Gray, 2019 (42).

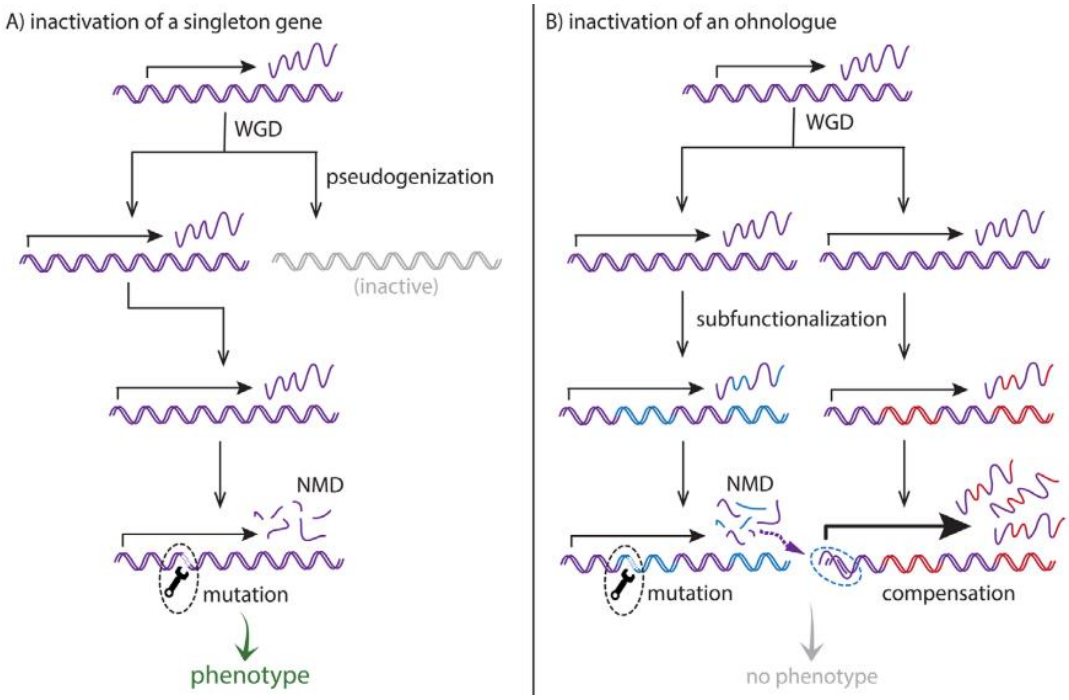
A) inactivation of a singleton gene
WGD
pseudogenization
(inactive)
NMD
mutation
phenotype
B) inactivation of an ohnologue
WGD
subfunctionalization
NMD
mutation
compensation
no phenotype

1.6 Canonical Wnt pathway

The Wnt pathway is an important signal transduction pathway heavily involved in embryonic development and adult tissue homeostasis. There are three pathways within Wnt signalling: canonical Wnt/β-catenin cascade, the non-canonical planar cell polarity pathway, and the noncanonical Wnt/Ca^{2+} pathway (49). Of the three, the canonical pathway is the best understood and is involved in tissue self-renewal, development, and cancer.

The Wnt pathway is activated by the binding of Wnt proteins to a Wnt receptor. Wnt ligand proteins are a family of lipid-modified glycoproteins that are secreted to enable cell-to-cell communications. Different Wnt ligands are known to be involved in different processes; Wnt3a is involved in hematopoietic stem cell proliferation in mouse embryonic development (50). The Wnt ligands bind to the Frizzled (Fz) transmembrane receptor, which then binds to another transmembrane receptor called low-density lipoprotein receptor-related protein, LRP5/6. This bound coreceptor complex recruits Dishevelled (Dvl) and leads to the phosphorylation of the cytoplasmic tail of LRP by glycogen synthase kinase 3β (GSK3β) and casein kinase 1(CK1). This recruits Axin to the complex, which prevents it from forming a β-catenin degradation complex. With its stabilization and accumulation, β-catenin localizes to the nucleus where it complexes with the transcription factor T cell factor/lymphoid enhancer factor (TCF/LEF) and promotes the transcription of Wnt target genes. In the absence of Wnt ligand binding, a degradation complex is formed with Axin as a scaffold. This complex is also composed of the tumor suppressor protein adenomatous polyposis coli (APC) and kinases GSK3β and CK1, which phosphorylate cytoplasmic β-catenin. This phosphorylated β-catenin is targeted for ubiquitination by an E3 ubiquitin ligase complex, and subsequently sent to the proteasome for rapid degradation. This rapid degradation of β-catenin in the cytoplasm prevents its translocation

to the nucleus and instead, nuclear TCF/LEF binds to Groucho, which inhibits transcription of Wnt target genes (49).

While USP4 and USP15 are both involved in the canonical Wnt pathway, they deubiquitinate different substrates. USP4 deubiquitinates Dvl, β-catenin, and TCF/LEF, while USP15 deubiquitinates APC and Smad3 (12, 24). As seen in Figure 3, USP4 has more substrates in the Wnt-stimulated pathway, while USP15 has more substrates in the unstimulated pathway.

Recently, Hwang *et al.* found a link between USP4 and lung adenocarcinoma through the canonical Wnt pathway (51). While the canonical Wnt pathway is known to be dysregulated in many cancers, there is growing evidence that it is critical in the development of non-small cell lung cancer (NSCLC). Wnt target genes including c-Myc are overexpressed in NSCLC (52). Also, aberrant expression of β-catenin is associated with epithelial-mesenchymal transition (EMT), an important part of metastasis (53). Hwang *et al.* demonstrated that brain metastatic lung adenocarcinoma cells had higher expression of β-catenin compared to their less invasive parental cells. They found that this increased expression was due to USP4, and when both USP4 and β-catenin were knocked down, there was a suppression of metastatic potential.

With the degree of association between the canonical Wnt pathway and our ohnologue pair of interest, this pathway would be ideal to monitor potential functional redundancy.

Figure 3. Canonical Wnt pathway with USP4 and USP15 substrates. The Wnt cellular signalling pathway substrates are depicted in the stimulated and unstimulated pathways. Downstream effector genes of the Wnt pathway are listed in the bottom right (Zeb1, LGR5 and TCF4). The dark blue arrows indicate USP4 substrates and the light blue arrows indicate USP15 substrates. This figure is adapted from Luo, K. (2016) Cold Spring Harb Perspect Biol. (54)

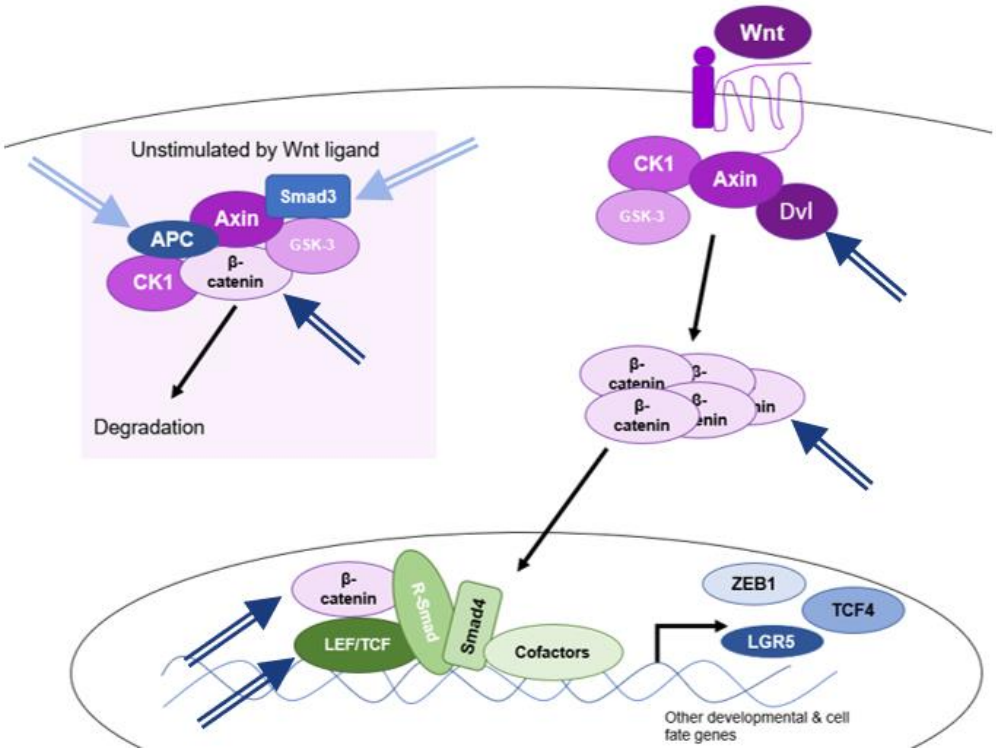
Wnt
Unstimulated by Wnt ligand
Smad3
Axin
APC
GSK-3
CK1
β-
catenin
Degradation
CK1
Axin
GSK-3
Dvl
β-
catenin
β-
catenin
β-
catenin
LEF/TCF
R-Smad
Smad4
Cofactors
ZEB1
TCF4
LGR5
Other developmental & cell
fate genes

1.7 Murine hematopoiesis

All the cellular components of blood are formed from hematopoietic stem cells (HSCs) and this process of development and differentiation is called hematopoiesis. Mammalian embryonic hematopoiesis consists of multiple waves of differentiation over time, first producing primitive erythroid linages, and later definitive erythroid lineages (55). Primitive erythropoiesis only occurs briefly in the earliest stages of development, and while their terminally differentiated large, nucleated cells persist during much of the gestational period, they are soon overtaken by the definitive erythroid cells. Primitive erythropoiesis is conserved amongst vertebrates, and any disturbance in the genes involved that results in a failure of this process is embryonic lethal very early in development. Definitive erythropoiesis begins at midgestation and the erythroid cells produced arise mainly from multipotent stem cells in the fetal liver. The fetal liver provides the microenvironment for these adult-type definitive enucleated erythroid cells to develop within erythroblastic islands (EBIs). These 3D structures have a central macrophage encircled by definitive erythroid cells at various stages of differentiation.

The location of hematopoiesis changes throughout murine embryonic development. The process begins during gastrulation around E6.5 with the formation of the mesoderm, which gives rise to both the primitive and definitive erythroid cells. Around E7.5, hematopoiesis takes place in the blood islands of the yolk sac. Between E7.5 and 9.5, definitive HSCs are formed in the para-aortic splanchnopleure. They then move to primarily the aorta-gonad-mesonephros (AGM) region around E10.5-11.5, as well as the placenta and major blood vessels. From E12.5-14.5, hematopoiesis moves to the developing fetal liver. Finally, around day 18.5, hematopoiesis takes places in the bone marrow, where it remains postnatally (55).

Canonical Wnt signaling is implicated in the regulation and differentiation of HSCs (50). Many canonical Wnt pathway components such as β-catenin and Wnt3a are expressed in the murine fetal liver at E12.5, a time of HSC expansion and differentiation. The Wnt3a ligand in particular appears to be very important for hematopoiesis at the fetal liver stage. When Wnt3a is knocked out, there are many developmental defects and death occurs at E12.5. Though there are other Wnt ligands expressed in the fetal liver, no other Wnt ligand can compensate for the loss of Wnt3a, which indicates that Wnt3a is likely the principle Wnt involved in liver HSC development (56).

Markers like c-Kit are widely used to identify HSCs, however more recently the membrane protein leucine-rich repeat-containing G-protein-coupled receptor 5 (LGR5) has been found to mark short-term HSCs during mouse embryonic development. LGR5 is known as a marker of intestinal crypt stem cells, and while it was recently found to also mark embryonic and fetal HSCs, it does not mark adult HSCs. Specifically, LGR5-expressing cells are found predominantly during the AGM and fetal liver stage of hematopoiesis (E11.5-13.5) (57). LGR5 is a downstream Wnt target gene, and it is one of the components of the receptor for R-spondins, which are stem cell growth factors and enhancers of Wnt signaling (58). Finally, LGR5 is expressed in lung adenocarcinoma, where it is positively correlated with stage in patients (59).

1.8 Hypothesis, Statement of Objectives and Significance

As discussed in the previous sections, USP4 and USP15 arose from an ancestral gene by whole genome duplication 500 million years ago, making them ohnologues. Though they share domain structure, enzymatic activity, and have roles in some of the same pathways including TGFβ and Wnt, they appear to have opposite effects in the outcomes of lung adenocarcinoma patients. To understand the roles of these ohnologues, we have acquired mice with an

inactivating mutation in either USP4 or USP15. Genetic crosses of such mice have determined that while mice deficient in either USP4 or USP15 are viable, those deficient in both are not. This observation has led to questions regarding compensation and functional redundancy in such an ohnologue pair. **We hypothesize that although USP4 and USP15 diverged in terms of substrates, sequence and structure, there may still be enough functional redundancy to allow one to perform the other's functions to a certain extent when deficient in one USP.** The work of my thesis research will be to use mice with inactivating mutations in either USP4 or USP15, and their progeny to study the extent of functional redundancy and subfunctionalization and investigate if this is the result of transcriptional compensation. Based on this rationale and hypothesis, there are three objectives:

I. Characterize Mendelian ratios of USP4Het and USP15Het intercrosses. Isolate and characterize mouse embryo fibroblasts (MEFs) from harvested embryos of all genotypes.

II. Investigate the cause of the lethality observed in embryos null in both USP4 and USP15 at embryonic day 12.5.

III. Investigate MEFs with USP4 and/or USP15 deficiency at the protein and RNA levels.

    A. Identify the cellular substrates and pathways in MEFs impacted during USP4 and/or USP15 deficiency.

    B. Investigate potential transcriptional compensation.

Completing the first objective will allow us to investigate any mild phenotypes in the mice of various genotypes, outside of the obvious lethal phenotype of the Null/Null genotype, indicating the extent of functional redundancy in our system. The characterization and subsequent immortalization of MEFs will allow for the investigation of cellular signaling

pathways indicated in the final objective. In the second objective, we will explore the cause of the embryonic lethality seen in the Null/Null genotype. This will provide us with an idea of which developmental processes and signaling pathways may be impaired in the absence of USP4 and USP15. The third objective will allow us to interrogate specific cellular pathway(s) that may be impacted in our system at the protein and RNA level. It will also allow for the investigation into transcriptional compensation, which we have recently postulated may be at play in DUB ohnologue systems.

As there is currently very little knowledge regarding the evolution of deubiquitinating enzymes, this study of the USP4 and USP15 gene ohnologues will contribute greatly in terms of the extent of their functional redundancy and in terms of the rewiring of molecular networks. Furthermore, USP4 is an attractive therapeutic target in cancer that many groups are attempting to target using inhibitors. However, a drug that also inhibited the highly related USP15 enzyme might have unexpected deleterious effects. We must better understand their roles specifically, but also more broadly, how molecular networks are remodelled after gene duplication.

CHAPTER 2: MATERIALS & METHODS

2.1 Mouse and embryo work

The animal work presented here was done using protocols approved by the Animal Care Committee of the University of Ottawa, and in accordance with the guidelines of the Canadian Council on Animal Care. Mice with inactivating mutations in *Usp4* or *Usp15* (gene-trap transgenic lines TF2497 and TF2834 respectively) were acquired from Taconic, Rensselaer, NY, United States, and were backcrossed to C57BL/6J mice for 10 generations in order to ensure a uniform genetic background. The genotype with respect to *Usp4* and *Usp15* were determined by polymerase chain reaction (PCR) from DNA isolated from tail or ear clippings using a T100 Thermal Cycler (Bio-Rad Laboratories Canada Inc, Mississauga, Ontario). The PCR reaction was prepared using REDExtract-N-Amp PCR ReadyMix (Sigma-Aldrich Canada Co., Oakville, Ontario, Canada) and primers are outlined in Table 1 (Invitrogen Canada Inc., Burlington, Ontario, Canada).

To isolate embryos, pregnant female mice were sacrificed from E10.5-12.5 (depending on the target age of the embryos). Immediately after sacrifice, the uterus was removed at the cervix and placed in a shallow dish of 1x phosphate-buffered saline (PBS). In a laminar flow hood, each embryo with placenta intact was removed from the uterus and placed in 1x PBS. At this point, each embryo was placed in a different dish with 1x PBS, where the placenta, outer membrane, and yolk sac were removed carefully. A piece of the tail was clipped for genotyping by PCR.

To culture mouse embryo fibroblasts (MEFs) at E12.5, the head and internal organs were removed, and the carcass was rinsed in another dish of 1x PBS. The rinsed carcass was then

placed in a new 10 cm tissue culture plate containing 5 mL of 0.25% trypsin/1mM EDTA. Using surgical scissors, the carcass was minced and then incubated at 37 °C for 10 minutes. Using a 5 mL plastic disposable pipet, the tissue was homogenized by vigorously pipetting 20-30 times. 5 mL of Dulbecco's Modified Eagle Medium (DMEM) media was added and the cell suspension was pelleted. The pelleted cells were resuspended in DMEM media and placed into tissue culture plates.

When the plates reached confluency, one plate was treated with 0.05% Trypsin/EDTA, pelleted, and resuspended in 1 mL of freezing media (90% fetal bovine serum, 10% DMSO). These live MEFs were placed in cryo-vials at -80 °C for at least 24 hours prior to storage in liquid nitrogen.

The rest of the tissue culture plates containing MEFs were used for growth curves (2.2), RNA isolation (2.4), Wnt treatment (2.6), or protein lysate isolation (2.7).

Table 1. Primer sequences for genotyping.

Gene of interest	Primer	Sequence
Usp4	Forward (Ex3)	5'-CCAGCAGCCTATTGTCAGAA-3'
	Reverse (In3)	5'-TCAGTACTTAGGGATCTCTGA-3'
	Reverse (Neo)	5'-AACCTGCGTGCAATCCATCT-3'
Usp15	Forward (TF2834-lower)	5'-GAGTACCTACAGGCACTTGAGACG-3'
	Forward (TF2834-upper)	5'-GGTTTGAAGGATAACGTAGGC-3'
	Reverse (LTR)	5'-ATAAACCCTCTTGCAGTTGCATC-3'

2.2 Cell culture and growth curves

Primary MEF cells were cultured at 37°C in DMEM media (Corning Life Sciences, Massachusetts, USA) supplemented with 10% fetal bovine serum. The primary MEFs were characterized by growth rate analysis. Growth curves were first performed at 20% O_2 and 37 °C, however this level of O_2 may be stressing the cells, which normally grow at a lower O_2 concentration *in vivo*. For this reason, growth curves were subsequently done at 4% O_2, a physiological level for many tissues. To set up the growth curve analysis, the primary MEFs were monodispersed with 0.05% Trypsin/EDTA (Corning Life Sciences, Massachusetts, USA) and resuspended in 5 mL of DMEM media. 1 mL was used to count the total number of cells with the Vi-Cell XR Cell Viability Analyzer (Beckman Coulter, Mississauga, Ontario, Canada). Cells were seeded at 20,000 cells/well, in triplicates, five times (for five days), in 6-well dishes. Cells were incubated at 37 °C for the indicated number of days, then monodispersed using trypsin. Cells were counted using the Vi-Cell counter. Mean cell counts and standard deviations were plotted against time using Excel.

In order to have cells for future experiments, primary MEFs derived from embryos of the genotypes Het/Het, Null/Null, Null/Het, Het/Null, and Wt/Wt were immortalized by serial passages according to a published protocol (60). Briefly, primary MEFs were counted using the Vi-Cell counter, and 3.8E5 cells were seeded in a T25 flask with 5 mL DMEM media. Cells were incubated at 37°C at 20% O_2 for 3-4 days. This was repeated and cell count at each passage was monitored until cells began to expand at a greater than 3-fold difference.

2.3 Immunohistochemistry

If the embryo was being isolated for whole-embryo sectioning and immunohistochemistry, then after a piece of the tail was clipped for genotyping, the rest of the embryo was kept intact. Each embryo was fixed in 10% formalin overnight, and then transferred to 70% ethanol. The embryo was embedded in paraffin, sectioned using a microtome, and mounted on slides.

A standard immunohistochemistry protocol was followed. Briefly, the tissue was deparaffinized in xylene and rehydrated in ethanol and water. After antigen retrieval with 10 mM sodium citrate buffer pH 6.0 in the microwave, endogenous peroxidase activity was quenched in methanol containing 3% H_2O_2 and the section was rinsed in PBS. Each sample was blocked using 2.5% normal goat serum and then incubated with the anti-LGR5 primary antibody (1:40) overnight (see Table 3 for antibody source). After rinsing with PBS, slides were incubated with biotin-conjugated secondary antibody (1:200 dilution) and then with avidin biotin complex solution (Biotinylated Goat Anti-Rabbit ABC Kit, Vector, California, USA). The slides were then incubated in 3,3′-Diaminobenzidine (KPL, Guelph, Canada) and counterstained in hematoxylin (Fisher Scientific, Ottawa, Canada). Finally, the slides were dehydrated and covered with glass coverslips. Slides were analyzed with the Olympus B Max and Leica model microscopes.

The whole embryos were also subject to Hematoxylin and Eosin (H&E) staining, which stained the nuclei blue and the cytoplasm red. Briefly, the tissue was deparaffinized and rehydrated, then stained in Harris Hematoxylin solution. The tissue was then counterstained in eosin Y solution (Sigma-Aldrich Canada Co., Oakville, Ontario, Canada), dehydrated and mounted for further analysis.

2.4 RNA extraction and reverse transcription polymerase chain reaction (RT-PCR)

Primary MEFs were cultured in a 10 cm plate for 4 days before being rinsed with PBS and scraped. Cells were centrifuged at 250 x g for 5 minutes and the supernatant was discarded. Total RNA was extracted from the cells using the GeneJET RNA Purification Kit (Thermo Scientific, Nepean, Ontario, Canada), as per the manufacturer's instructions. When starting with liver tissue, it was disrupted and homogenized using a rotor-stator homogenizer, and then RNA was extracted from the suspension as per the manufacturer's instructions. RNA concentration was determined using the Nanodrop (Perkin Elmer Optoelectronics, Woodbridge, Ontario, Canada).

Reverse transcription polymerase chain reaction (RT-PCR) was carried out using the MyTaq One-Step RT-PCR Kit (BioLine, Toronto, Ontario, Canada). In a PCR tube, kit components 2x MyTaq One-Step Mix, reverse transcriptase enzyme, RiboSafe RNase inhibitor, and DEPC-H_2O were combined along with 400 nM each of forward and reverse primers. Primer sequences and sources are described in Table 2. Reverse transcription and amplification reactions were carried out according to kit conditions in a T100 Thermal Cycler (Bio-Rad Laboratories Canada Inc, Mississauga, Ontario). A 1.1% agarose gel was prepared, and PCR products were run at 100 V. Gel was visualized using the Epi Chemi II Darkroom (UVP Laboratory Products, California, USA).

Table 2. mRNA-specific primer sequences and their sources

Target transcript	Sequence	Source
Lgr5	Forward: 5'-ACCCGCCAGTCTCCTACATC-3' Reverse: 5'-GCATCTAGGCGCAGGGATTG-3'	Munoz *et al.* 2012 (61)
Usp4	Forward: 5'-CCTCGTGAACTCCTGTGG-3' Reverse: 5'-AGGCTTCGGGTCTCACTG-3'	Previous student
Usp15	Forward: 5'-TCCTGGACCCATCGATAACTCTG-3' Reverse: 5'-CATACCCTGTTCTACCACCTTTC-3'	Feng *et al.* 2014 (62)*

*Note: the primers in the article are for human, and one base was corrected in each For and Rev to match mouse RNA exactly.

2.5 Quantitative polymerase chain reaction (qPCR)

The RNA isolation protocol described in 2.4 were repeated to produce starting material for all qPCR reactions here. The qPCR reaction was prepared using the iTaq Universal SYBR Green One-Step Kit, which performs the reverse transcription reaction followed by the quantitative PCR reaction in one step (Bio-Rad Laboratories Canada Inc, Mississauga, Ontario, Canada). The same primers generated for RT-PCR, described in Table 2 were used for qPCR, after standard curves were performed, and efficiency plots were made to ensure the efficiency of the primers. Amplicons were detected in triplicate using the Applied Biosystems 7500 Fast Real-Time PCR System (Thermo Scientific, Nepean, Ontario, Canada). Raw C_t values were identified using the AB software. ΔC_t values were calculated by subtracting the *Ppia* mRNA C_t values from the mRNA of interest (*Usp4* or *Usp15*) C_t values. The $\Delta\Delta C_t$ values (relative mRNA abundance) were calculated by subtracting the ΔC_t values of the Wt/Wt RNA from the ΔC_t values of the RNA from the genotype of interest. The relative quantification (RQ) values were calculated using the equation $2^{-\Delta\Delta Ct}$.

2.6 Wnt stimulation and optimization

In order to get a full picture of the activity of the canonical Wnt pathway in the MEFs, both the unstimulated and stimulated pathways were examined. Recombinant mouse Wnt3a protein was prepared at 1.0 mg/mL in PBS supplemented with 0.25% bovine serum albumin (Abcam, Cambridge, UK). To determine the optimal Wnt3a stimulation and harvest time, Wnt3a was added to fresh DMEM media at 0 ng/mL, 50 ng/mL, 100 ng/mL, and 200 ng/mL. NIH3T3 immortalized mouse fibroblast cells were used for optimization and the Wnt3a-supplemented media was added to a plate of cells approximately 80% confluent. After 24 hours and 48 hours of incubation (harvest times were based on published protocols) at 37°C and 4% O_2, cells were

scraped, protein lysate was extracted, and western blots were done (as will be described in 2.7). Optimal expression of β-catenin was used to determine the optimal Wnt3a concentration and harvest time- 100 ng/mL and harvest after 24 hours.

Primary MEFs of each genotype of interest were cultured for 3 days prior to being stimulated with 100 ng/mL of Wnt3a DMEM media and harvested after 24 hours.

2.7 Protein extraction and western blot analysis

Primary MEFs were cultured in a 10 cm plate for 4 days before being rinsed with PBS and scraped. Cells were centrifuged at 300 rpm for 5 minutes and the supernatant was discarded. Cells were lysed using a protein lysis buffer (20mM Tris-HCl pH 7.5, 150nM NaCl, 1% Nonidet P-40, 2 mM EDTA, 1% glycerol), supplemented with 2mM sodium fluoride (NaF), 2mM sodium pyrophosphate (NaPPi), 50 μM sodium orthovanadate ($NaVO_4$), 1 mM phenylmethylsulfonyl fluoride (PMSF) and 1X protease inhibitor cocktail (Roche Applied Science, Laval, Quebec, Canada). Cell lysates were sonicated 3 times for 10 seconds each, chilling them on ice between sonications. The cell lysates were pelleted and the supernatants transferred to new chilled tube. The protein concentrations were determined using the Bradford protein assay (Bio-Rad Laboratories Canada Inc, Mississauga, Ontario, Canada) and the absorbance was read at 595 nm using a spectrophotometer.

Protein lysates were prepared with SDS sample buffer (0.5M Tris HCl pH 6.8, 40% glycerol, 10% SDS, 1% bromophenol blue, 5% β-mercaptoethanol). Samples were heated to 95 °C for 5 minutes, with the exception of blots to be probed with the LGR5 antibody, which were heated to 70°C for 20 minutes. Protein samples (20 μg/lane of cell lysates or 30 μg/lane for LGR5 blots) were resolved on a 4-15% TGX Tris-Glycine Stain-free gel by SDS-PAGE (Bio-

Rad Laboratories Canada Inc, Mississauga, Ontario, Canada). After running, the gel was activated for 45 seconds using the “Stain Free Gel” option on the ChemiDoc Imaging System (Bio-Rad Laboratories Canada Inc, Mississauga, Ontario). The resolved proteins were transferred to a low fluorescence polyvinylidene fluoride (PVDF) membrane using the Trans-Blot Turbo RTA Mini LF PVDF Transfer Kit (Bio-Rad Laboratories Canada Inc, Mississauga, Ontario, Canada). An image of the transferred blot was taken using the “Stain Free Blot” option on the ChemiDoc. This is an image of the total loaded protein which would be used for normalization by the ImageLab software. Membrane was incubated 1 hour in 5% skim milk in TBST (10mM Tris-HCl pH 7.6, 150mM NaCl and 0.05% Tween-20) at room temperature. Then the membrane was incubated in each respective primary antibody diluted in 5% skim milk in TBST and incubated overnight at 4°C or at room temperature for 1 hour (see Table 3 for antibody dilutions). Membranes were wash 3 times for 5 minutes each in TBST, then incubated for 1 hour at room temperature in corresponding secondary antibody diluted in 5% skim milk in TBST. Finally, the membrane was washed in the same way, then visualized using the Immobilion Forte Western HRP Substrate (Millipore, MA, USA).

Table 3. Antibodies for western blot, immunoprecipitation, and immunohistochemistry

Antibody	**Company**	**Western blot dilution**
Zeb1	Bethyl Laboratories Inc.	1:1000
β-catenin	Abcam	1:4000
TCF4	Abcam	1:500
β-actin	Sigma	1:10 000
APC	Abcam	1:100
LGR5	Abcam	1:750
USP4	Cell Signaling Technology	1:1000

2.8 Immunoprecipitation

Cell lysates from Wnt-stimulated Wt/Wt MEFs and unstimulated Wt/Wt MEFs were immunoprecipitated. After quantifying the total protein using the Bradford Protein Assay (Bio-Rad Laboratories Canada Inc, Mississauga, Ontario, Canada), 400 µg of protein were diluted with RIPA Buffer (50mM Tris-HCl, pH 7.4, 1% NP-40, 0.5% Na-deoxycholate, 0.1% SDS, 150mM NaCl, 2mM EDTA, 50mMNaF) supplemented with protease inhibitors. The protein lysate was added to Sepharose ProtA beads (GE Healthcare, Piscataway, NJ, USA) and LGR5 primary antibody (1:20 dilution), and the slurry was incubated on a rotator at 4°C for 1.5 hours. The slurry was spun down to remove the supernatant and washed 4 times with NETN buffer (50mM Tris-HCl, pH 7.4, 1% Triton X-100, 1mM EDTA, 200mM NaCl, 10% glycerol). Beads were dried using a G30 needle and resuspended in assay buffer. To remove the protein of interest from the beads, the samples were heated at 70 °C for 20 minutes (as per LGR5 antibody instructions), spun down and the supernatant was saved. The remaining beads fraction was resuspended again in assay buffer and heated at 95 °C for 5 minutes, spun down, and the supernatant reserved. The input (to immunoprecipitation reaction), the immunoprecipitated protein (after 70 °C heating for 20 minutes) and any remaining immunoprecipitated protein (after extra 95 °C heating for 5 minutes) were run on a SDS-PAGE gel and transferred to a nitrocellulose membrane, as described in 2.7. The membrane was autoclaved in the wet cycle for 45 minutes to expose the ubiquitin epitope. The membrane was blocked in 20% BSA in TBST solution and was probed with an anti-ubiquitin primary antibody (Santa Cruz Biotechnology, Dallas, USA) and secondary antibody (1:10 000 dilution), before being visualized using the ECL substrate. The blot was then stripped, and the empty blot was visualized using the ECL substrate. Finally, the blot was probed with anti-LGR5 primary antibody, as described in 2.7.

CHAPTER 3: RESULTS

3.1 Characterization and immortalization of MEFs

Mice with inactivating mutations in USP4 and USP15 were crossed and it was determined that while mice deficient in either USP4 or USP15 are viable, those deficient in both (Null/Null) are not. However, embryos of the Null/Null genotype survive until approximately embryonic day 12.5 (Coulombe, Zachariah, Gray, unpublished). I harvested embryos of all USP4 and USP15 genotype combinations at embryonic day 12.5. Primary mouse embryo fibroblasts (MEFs) of the genotypes Het/Het (heterozygous in USP4, heterozygous in USP15), Null/Null, Null/Het and Het/Null were isolated and cultured as described (one primary MEF culture per genotype). The primary MEFs were characterized by growth rate analysis by counting the total number of cells at the indicated time point after seeding equally. Growth curves were first performed at 20% O_2 and 37 °C, however this level of O_2 may be stressing the cells, which normally grow at a lower O_2 concentration *in vivo* (63). For this reason, growth curves were subsequently done at 4% O_2. The Null/Het MEFs consistently had the highest growth rate, followed by Het/Het, then Het/Null, and finally, Null/Null (Figure 4A).

The primary Het/Het, Null/Null, Null/Het, and Het/Null MEFs were spontaneously immortalized through serial passage over the course of several months in order to be used as cell lines for future experiments (Figure 4B). Cultures were maintained at 20% O_2 and reached a crisis point where most cells stopped dividing, from which a few immortalized clones emerged. It is generally accepted that when the cell numbers increase about 3-fold with respect to the number of cells inoculated, during each 3-4 day passage at high O_2, the cells are sufficiently immortalized (60). Three batches of cells of each genotype were frozen and placed in liquid nitrogen storage for later use.

Figure 4. Growth curve and immortalization of MEFs. (A) Primary MEFs of all genotypes were seeded with 2 E+04 cells in triplicate in 6-well plates, and then incubated at 37 °C and in 4% O_2. Cells were counted at each indicated time point using the ViCell Cell Viability Analyzer. Null/Het MEFs have the highest growth rate, followed by Het/Het, then Het/Null, and Null/Null. **(B)** Primary MEFs of each indicated genotype were immortalized over the course of several passages in the 20% O_2 incubator. Note that Null/Null MEFs were immortalized during a previous immortalization attempt that was not recorded.

(A)

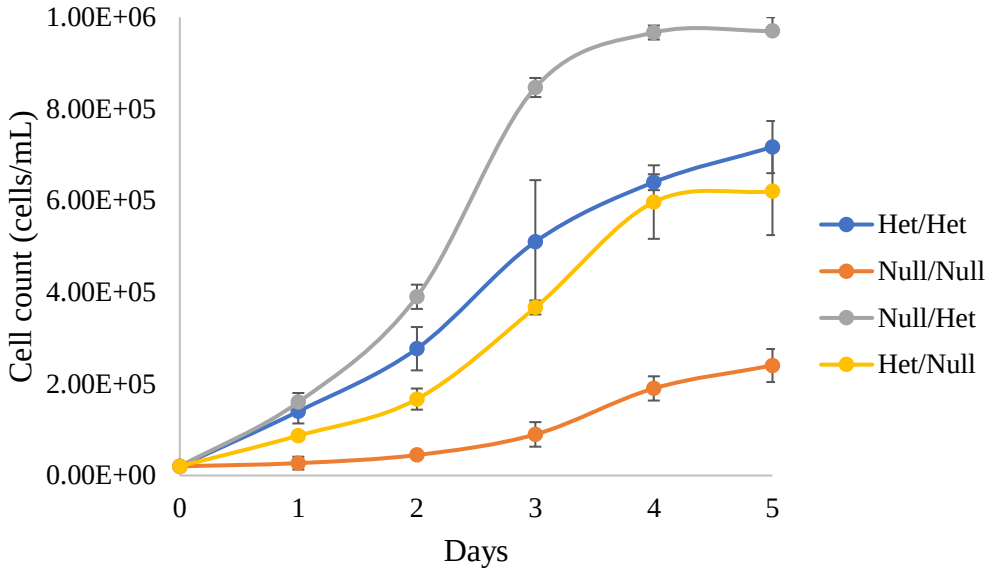
1.00E+06
8.00E+05
6.00E+05
4.00E+05
2.00E+05
0.00E+00
Cell count (cells/mL)
0
1
2
3
4
5
Days
Het/Het
Null/Null
Null/Het
Het/Null

(B)

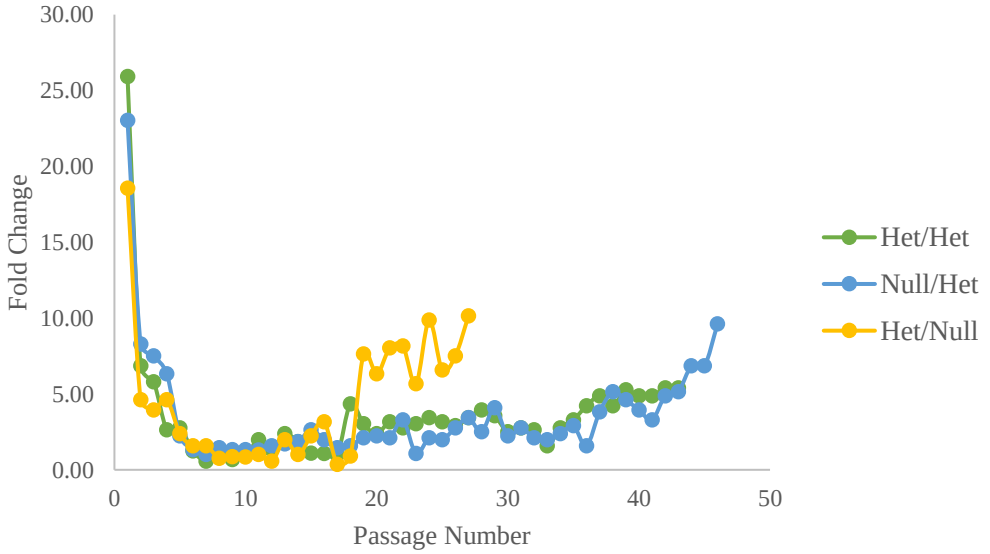
30.00
25.00
20.00
15.00
10.00
5.00
0.00
Fold Change
0
10
20
30
40
50
Passage Number
Het/Het
Null/Het
Het/Null

3.2 Sub-Mendelian ratios of USP4 and USP15 intercross and other observed phenotypes

When the initial mice with inactivating mutations in either USP4 or USP15 were acquired, they were backcrossed to C57BL/6J mice for 10 generations in order to ensure a uniform genetic background for our purposes. This allowed for the analysis of Mendelian transmission for both USP4 and USP15 separately. When mice heterozygous for the gene of interest are bred together, Mendelian laws of inheritance state that about 25% of progeny will be wildtype, 50% will be heterozygous, and 25% will be null. Figure 5A encompasses the results of n=292 and demonstrates that with respect with USP4, Mendelian transmission occurs such that 24% of the progeny are wildtype, 49% are heterozygous, and 27% are null. However, Figure 5B shows that when USP15 is considered, sub-Mendelian ratios were achieved because while 23% were wildtype, 63% were heterozygous and 13% were null (n=259).

Furthermore, it was observed that the USP15-null mice appeared smaller than the USP15-het or USP15-wildtype mice. These mice were weighed over the course of several weeks and it was observed that while the difference in weight was particularly noticeable and persistent in the male mice, the females appeared to catch up. Figure 5C shows the weights of a cohort of male mice at 5, 6, 7 and 9 weeks. It is clear that the null mice (in grey) are smaller in weight than the others. When taking all the male mice that were weighed together at each timepoint and looking at their weights as a percentage of the average heterozygous male weights, this trend is conserved (Figure 5D). However, when taking all the female mice that were weighed together at each timepoint and looking at their weights as a percentage of the average heterozygous female weights, it can be seen that while there is an initial difference between heterozygous and null females, the null females catch up by about 8 weeks (Figure 5E). Note that not enough wildtype females were weighed to be included in this analysis.

As was previously published by our group, when mice heterozygous for inactivating mutations in USP4 and USP15 were mated, none of the resulting progeny were Null/Null, indicating this genotype is embryonic lethal. This result was statistically significant by binomial analysis ($p = (15/16)^{166} = 0.000022$) (12). However, these results were published in 2015, prior to the USP4 and USP15 mice being backcrossed to C57BL/6J mice for 10 generations. Once this was completed, we saw the same overall result: the Null/Null genotype is embryonic lethal with a high degree of confidence by binomial analysis ($p = (15/16)^{137} = 0.000144$) (Table 4). Interestingly, other trends emerged as well. When USP15 is null, only 2% of the progeny are USP4-Het and 3% are USP4-Wt. This is less than the expected Mendelian ratios of 12.5% and 6.25%, respectively (Table 4, in parentheses). Conversely, when USP4 is null, 20% of the progeny are USP15-Het, which is more than the expected Mendelian ratio of 12.5%. While all the mice that are not Null/Null are viable, there is a clear skewing of Mendelian ratios.

Figure 5. Sub-Mendelian ratios and other observed phenotypes. For each of the following graphs, the Wt genotype is represented in blue, Het genotype in orange, and Null genotype in grey. **(A)** Mice with an inactivating mutation in USP4 were mated (n=292) and pup genotype was determined by polymerase chain reaction analysis. Expected Mendelian ratios for such a cross are 25% Wt, 50% Het, and 25% Null. **(B)** Mice with an inactivating mutation in USP15 were mated (n=259) and pup genotype was determined by polymerase chain reaction analysis. Expected Mendelian ratios for such a cross are 25% Wt, 50% Het, and 25% Null. **(C)** A cohort of USP15 (Wt, Het, or Null) male mice were weighed at 5, 6, 7, and 9 weeks to monitor growth. USP15-null mice were consistently smaller than their Het or Wt counterparts over the time studied. **(D)** Different USP15 males were weighed at different times, therefore all the male mice that were weighed together at each timepoint were averaged and then presented as a percentage of the average heterozygous male weights. These percentages of average heterozygous male weights are presented at 4, 6, 8, 10, and 12 weeks. **(E)** Different USP15 females were weighed at different times, therefore all the female mice that were weighed together at each timepoint were averaged and then presented as a percentage of the average heterozygous female weights. These percentages of average heterozygous female weights are presented at 4, 6, 8, 10, and 12 weeks. Note that there were not sufficient Wt female mice weighed to be included.

(A)

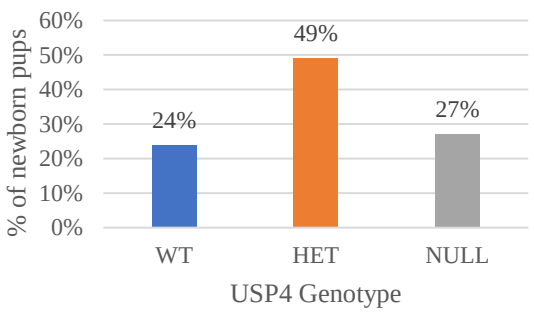
60%
50%
40%
30%
20%
10%
0%
% of newborn pups
49%
24%
27%
WT
HET
NULL
USP4 Genotype

(B)

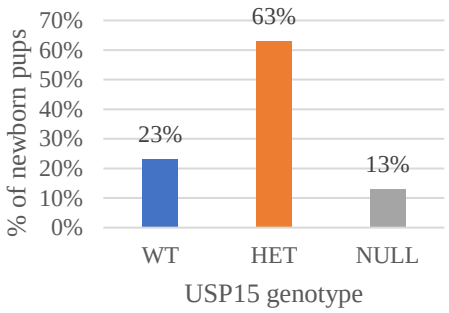
70%
60%
50%
40%
30%
20%
10%
0%
% of newborn pups
63%
23%
13%
WT
HET
NULL
USP15 genotype

(C)

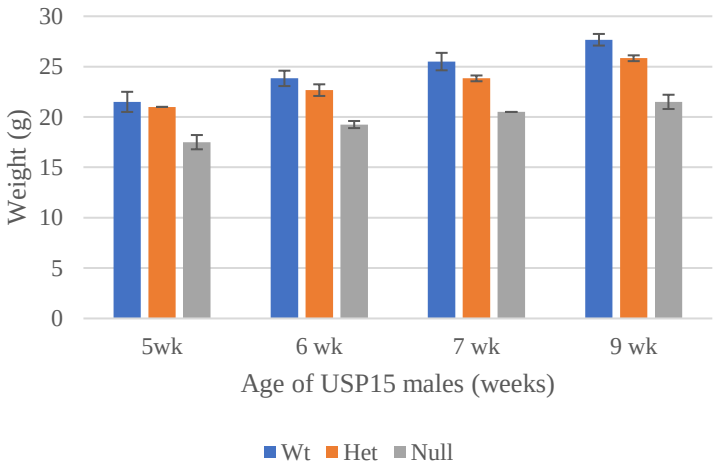
30
25
20
15
10
5
0
Weight (g)
5wk
6 wk
7 wk
9 wk
Age of USP15 males (weeks)
Wt
Het
Null

(D)

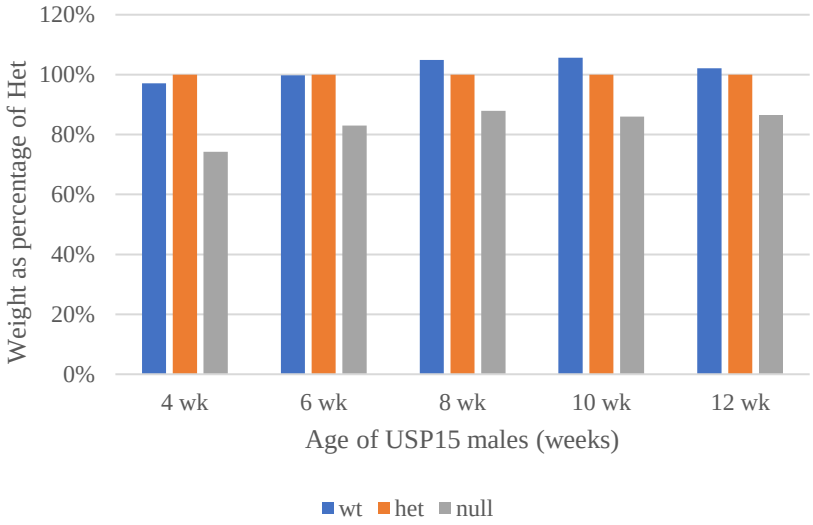
120%
100%
80%
60%
40%
20%
0%
Weight as percentage of Het
4 wk
6 wk
8 wk
10 wk
12 wk
Age of USP15 males (weeks)
wt
het
null

(E)

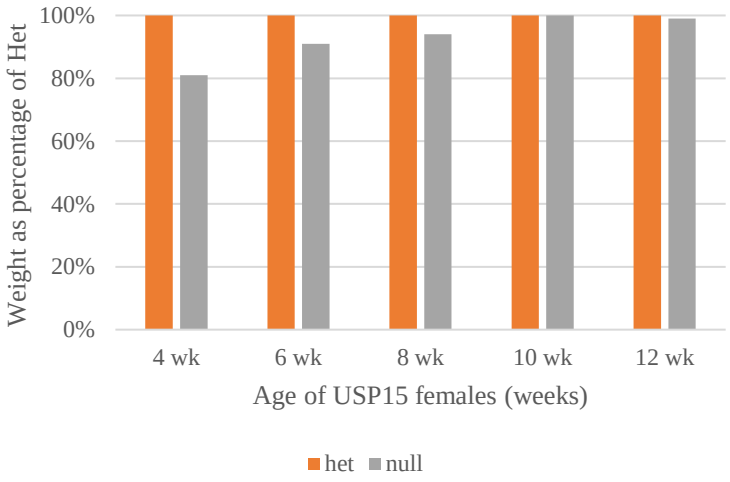
100%
80%
60%
40%
20%
0%
Weight as percentage of Het
4 wk
6 wk
8 wk
10 wk
12 wk
Age of USP15 females (weeks)
het
null

Table 4. Progeny from USP4^{Het}xUSP15^{Het} intercross.

		USP15		
		Wt	**Het**	**Null**
USP4	**Wt**	9% (6.25%)	19% (12.5%)	3% (6.25%)
	Het	12% (12.5%)	28% (25%)	2% (12.5%)
	Null	7% (6.25%)	20% (12.5%)	0% (6.25%)

Percentages of progeny with each indicated genotype from a USP4HetxUSP15Het intercross are shown here. The percentage values in parentheses are the expected Mendelian ratios.

3.3 Null/Null embryos at embryonic day 12.5 (E12.5)

While there are no Null/Null progeny born, they do survive *in utero* until approximately embryonic day 12.5 (E12.5). Null/Null embryos at this stage are consistently smaller than mice of any other genotype and lack the characteristic red spot in their torso (Figure 6A). We have also isolated embryos at earlier stages (E10.5 and E11.5) and the Null/Null embryos are noticeably smaller at these earlier stages as well (data not shown).

Embryo sections of both Wt/Wt and Null/Null genotypes were stained with a hematoxylin and eosin (H&E) stain to reveal the most obvious difference between the embryos is a liver deficit (Figure 6B). While wildtype fetal livers at E12.5 have sufficient structure and cohesion to be easily isolated from the rest of the embryo, Null/Null fetal livers lack structural integrity and cannot be clearly separated from the surrounding tissue. At this stage in development, hematopoiesis takes place in the fetal liver, which gives it the characteristic red colour in contrast to the translucent pink-white hue of the rest of the embryo (55). Previously, to look for evidence of hematopoiesis, the wildtype and null embryos were stained with c-Kit, a commonly used marker of hematopoiesis (data not shown). The wildtype liver had many hematopoietic cells in different stages of hematopoiesis- some were nucleated, and some were enucleated. The null liver had little to no c-Kit staining and lacked the structure evident in the wildtype liver. This c-Kit staining provides evidence that there may be a hematopoietic defect in the Null/Null mice.

Figure 6. Null/Null embryos at E12.5 are smaller with underdeveloped livers. (A) Embryos at day 12.5 are pictured with the following genotypes: Het/Het, Null/Het, Het/Null, and Null/Null. **(B)** The wildtype (left panel) and null (right panel) embryos were embedded in paraffin, sectioned and then stained with hematoxylin and eosin. The livers have been indicated by a black outline. A portion of the tail is missing because it was cut at the time of isolation for genotyping analysis by PCR.

(A)

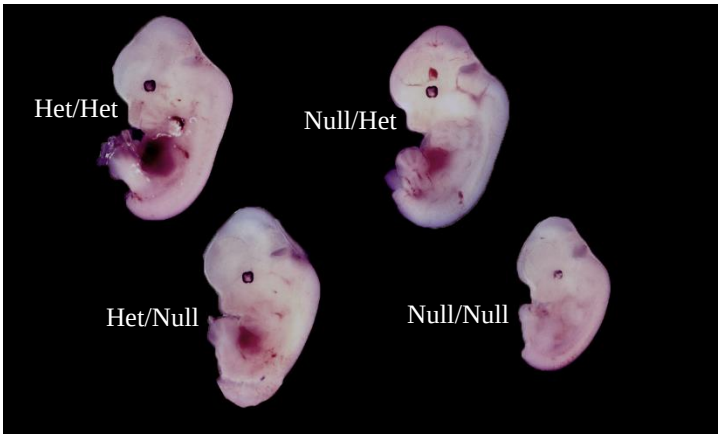

(B)

3.4 LGR5 is a marker of hematopoiesis in the fetal liver

Prior to my tenure in the Gray lab, MEFs null in USP4 were isolated and cultured for DNA microarray analysis. From this data, genes that were most significantly downregulated in the USP4-null MEFs compared to USP4-wildtype MEFs included *Usp4* (as expected) and *Lgr5* (Table 5). Genes that were upregulated in the USP4-null MEFs compared to USP4-wildtype MEFs are described in Table 6, however they did not show the same magnitude of fold change compared to the two most downregulated genes in Table 5. Since *Lgr5* is the second most downregulated gene in USP4-null MEFs after the expected *Usp4*, it became an interesting target to analyze.

Leucine-rich repeat-containing G-protein-coupled receptor 5 (LGR5)-expressing cells are found predominantly during the aorta-gonad-mesonephros (AGM) and fetal liver stage of hematopoiesis (E11.5-13.5), and LGR5 is a Wnt target gene (57, 58). First, we had to ensure that there is expression of LGR5 in the fetal liver as the literature suggests. Primers for RT-PCR were ordered based on previously published sequences for mouse LGR5, along with USP4 and USP15 (61, 62). RT-PCR was done on wildtype fetal liver at E12.5 with LGR5, USP4, and USP15 primers and expression of each target transcript was confirmed (Figure 7A).

Sagittal sections in paraffin of the wildtype and null E12.5 embryos were stained with the LGR5 antibody to analyze hematopoiesis (Figure 7B). As seen in the H & E staining of the same embryos, the Null/Null embryos have small livers with very little LGR5 staining. In contrast, the wildtype embryos have significant LGR5 staining throughout the liver.

From this evidence, the obvious next step would be to isolate Null/Null fetal livers to analyze them for LGR5 expression. Unfortunately, due to the overall small size of the embryo and lack

of structural integrity of these E12.5 Null/Null livers, we were unable to isolate their livers for this analysis. Therefore, we had to rely on the next best thing- E12.5 livers with the USP4-null or USP15-null genotype.

To study expression of LGR5 in these livers, RNA was extracted, and qPCR was performed. The same LGR5 primers that were used for RT-PCR were used for qPCR. Standard curves were performed, and efficiency plots were made to ensure the efficacy of the primers (data not shown). The same was done for *Ppia*, a standard housekeeping gene to be used as an endogenous control (64). The ΔΔCt method was employed to analyze the data and each sample was compared to a reference sample of Wt/Wt RNA. Interestingly, the USP15-null (Wt/Null) livers had less expression of LGR5 than their wildtype counterparts (Figure 7C). Conversely, the USP4-null (Null/Wt) livers had more expression of LGR5 than their wildtype counterparts.

Sections of the E12.5 USP15-null and USP4-null embryos were stained with the LGR5 antibody and the qPCR results were recapitulated- the USP15-null livers had less expression of LGR5 than the USP4-null livers (Figure 7D). This indicates that what qPCR captured at the transcriptional level was the same at the protein level. The reduction in LGR5 protein in null mice is therefore explicable through the reduction of mRNA levels rather than through post-translational effects (a plausible mechanism given the regulation of protein levels by deubiquitinating enzymes such as USP4 and USP15).

At this point it was clear that the Null/Null embryos have small livers and defective hematopoiesis- however, we did not know if the HSCs arrived at the fetal liver already defective, or if the lack of a properly structured liver makes the HSCs defective. To investigate this question, we isolated embryos at E10.5 and E11.5. Hematopoiesis occurs in the transient AGM at approximately E10.5-E11.5, and is seeded in the liver around E11.5, and then fully moves to

the liver between E12.5-E14.5 (55). This process appears to be normal in the wildtype E11.5 and E12.5 AGMs and livers (Figure 7E). As expected, there are fewer LGR5+ cells in the AGM at E12.5 than E11.5 due to HSC movement to the liver.

Due to the extremely small size of the E10.5 embryos, we were unable to get any usable sections for IHC. However, we were able to stain E11.5 embryos with the LGR5 antibody (Figure 7F). The wildtype E11.5 embryos have a normal-appearing liver and AGM, with many cells positive for LGR5 in both organs, as seen in Figure 7E. The Null/Null E11.5 embryo has a slightly wider-than-normal AGM with several cells positive for LGR5. The Null/Null E11.5 liver is small, has several cells positive for LGR5, but also has some damage, indicated by the arrow (Figure 7G, left panel). This damage appears to worsen by E12.5, and there are fewer cells positive for LGR5 (Figure 7G, right panel).

Finally, by using an online tool that provides a single cell RNA-seq SPRING plot of human hematopoietic progenitors, we saw that USP15 was expressed more than USP4 in these hematopoietic progenitors (Figure 7H, middle and right panels) (65). Figure 7H left panel maps out sections of the plot that correspond to transcriptional states associated with early lineage commitment. For instance, the bottom left region represents the erythroid lineage.

Table 5. DNA microarray of downregulated gene transcripts in USP4-null MEFs.

Number	Gene symbol	Gene title	log2 (fold change)	Linear fold change
1	Usp4	ubiquitin specific peptidase 4	-3.88315	-14.75518
2	Lgr5	leucine rich repeat containing G protein coupled receptor 5	-2.35974	-5.132779
3	Qpct	glutaminyl-peptide cyclotransferase	-1.92889	-3.807621
4	Syt13	synaptotagmin XIII	-1.58554	-3.001201
5	Pcsk9	proprotein convertase subtilisin/kexin type 9	-1.55926	-2.947026
6	Bcl11b	B cell leukemia/lymphoma 11B	-1.46205	-2.754996
7	Igsf10	immunoglobulin superfamily, member 10	-1.46126	-2.753487
8	Itga4	integrin alpha 4	-1.45097	-2.733918
9	Id4	inhibitor of DNA binding 4	-1.42907	-2.692731
10	Dhrs9	dehydrogenase/reductase (SDR family) member 9	-1.37332	-2.590661
11	Igfbp5	insulin-like growth factor binding protein 5	-1.36587	-2.577317
12	Irx1	Iroquois related homeobox 1	-1.35228	-2.553153
13	Ldb2	LIM domain binding 2	-1.3417	-2.534498
14	Ptprz1	protein tyrosine phosphatase, receptor type Z, polypeptide 1	-1.32796	-2.510474
15	Pdgfra	platelet derived growth factor receptor, alpha polypeptide	-1.32436	-2.504218
16	Gfra1	glial cell line derived neurotrophic factor family receptor alpha 1	-1.3159	-2.489576
17	C1qtnf 3	C1q and tumor necrosis factor related protein 3	-1.3122	-2.483199
18	Kcne4	potassium voltage-gated channel, Isk-related subfamily, gene 4	-1.27697	-2.423295
19	Jag1	jagged 1	-1.27361	-2.417658
20	Dpt	dermatopontin	-1.26357	-2.400891

Table 6. DNA microarray of upregulated gene transcripts in USP4-null MEFs.

Number	Gene symbol	Gene title	log2 (fold change)	Linear fold change
1	Eltd1	EGF, latrophilin seven transmembrane domain containing 1	2.18475	4.54648
2	Des	desmin	2.08622	4.24634
3	Penk	preproenkephalin	2.03986	4.112056
4	Nt5e	5 nucleotidase, ecto	1.98633	3.962278
5	Fgf2	fibroblast growth factor 2	1.92684	3.802215
6	Ifi44	interferon-induced protein 44	1.86061	3.631612
7	Mstn	myostatin	1.80261	3.488508
8	Arhgap36	Rho GTPase activating protein 36	1.76592	3.400908
9	Msln	mesothelin	1.73184	3.321512
10	Ndnf	neuron-derived neurotrophic factor	1.72057	3.295666
11	Angptl7	angiopoietin-like 7	1.66788	3.177473
12	Luzp2	leucine zipper protein 2	1.51674	2.861437
13	Serpinb6b	serine (or cysteine) peptidase inhibitor, clade B, member 6b	1.4762	2.78215
14	Rasgrp3	RAS, guanyl releasing protein 3	1.46198	2.754862
15	Plac8	placenta-specific 8	1.412	2.661058
16	Enpp2	ectonucleotide pyrophosphatase/phosphodiesterase 2	1.34989	2.548927
17	Bckdhb	branched chain ketoacid dehydrogenase E1, beta polypeptide	1.32036	2.497284
18	Ccl9	chemokine (C-C motif) ligand 9	1.28628	2.438983
19	Npr3	natriuretic peptide receptor 3	1.27022	2.411983
20	Nrn1	neuritin 1	1.25119	2.380377

Figure 7. LGR5 expression may explain hematopoietic defect. (A) To ensure expression of LGR5, USP4, and USP15 in the fetal murine liver at the stage of interest, RNA was extracted from E12.5 wildtype embryo livers. Reverse transcription polymerase chain reaction was done with previously published primers for murine LGR5, USP4, and USP15, either with (+) or without (-) the reverse transcriptase enzyme to ensure any amplification was truly of the mRNA transcript of interest. Each of LGR5, USP4 and USP15 were all confirmed to be expressed in fetal livers. **(B)** Images of sagittal paraffin sections of E12.5 Wt/Wt (left) and Null/Null (right) embryos stained with LGR5 taken on the scanning microscope (not to scale). **(C)** Quantitative polymerase chain reaction in triplicate was performed on wildtype, USP15-null (Wt/Null) and USP4-null (Null/Wt) fetal livers to analyze LGR5 expression. USP15-null livers had less expression than USP4-null livers. **(D)** Immunohistochemistry was performed on wildtype, USP15-null and USP4-null E12.5 embryo sections, staining for LGR5. USP15-null livers had less LGR5-positive cells than USP4-null livers. **(E)** E11.5 (top) and E12.5 (bottom) AGM and livers from wildtype embryos stained with LGR5. This demonstrates how at E11.5, hematopoiesis primarily takes place in the AGM, and then moves to primarily take place in the liver at E12.5. **(F)** Images of sections of E11.5 Wt/Wt (left) and Null/Null (right) embryos stained with LGR5 taken on the scanning microscope (not to scale). **(G)** Fetal livers of Null/Null embryos at E11.5 (left) and E12.5 (right) stained with LGR5. Red arrows show damage in E11.5 liver, whereas damage is ubiquitous throughout the E12.5 liver. **(H)** SPRING plot showing USP15 (middle) is more highly expressed in human hematopoietic progenitors than USP4 (right). The left panel designates each transcriptional state with the early lineage they are aligned with: E, erythroid cells; Meg, megakaryocytes; BaP, basophil progenitors; P, early progenitor cells; Ly, lymphoid T/B/NK cells; DC, dendritic cells; M, monocytes, N, neutrophils. (65)

(A)

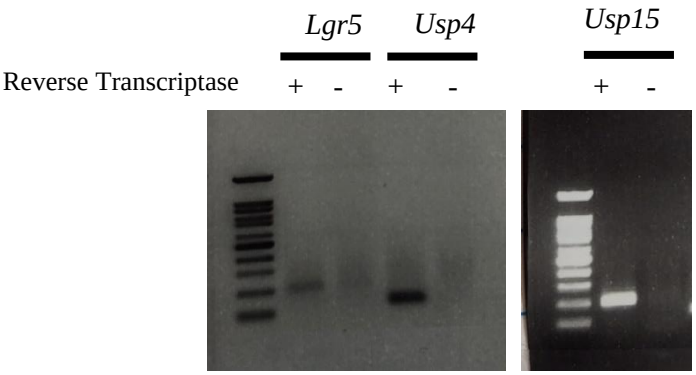
Lgr5
Usp4
Usp15
Reverse Transcriptase
+ - + -
+ -

(B)

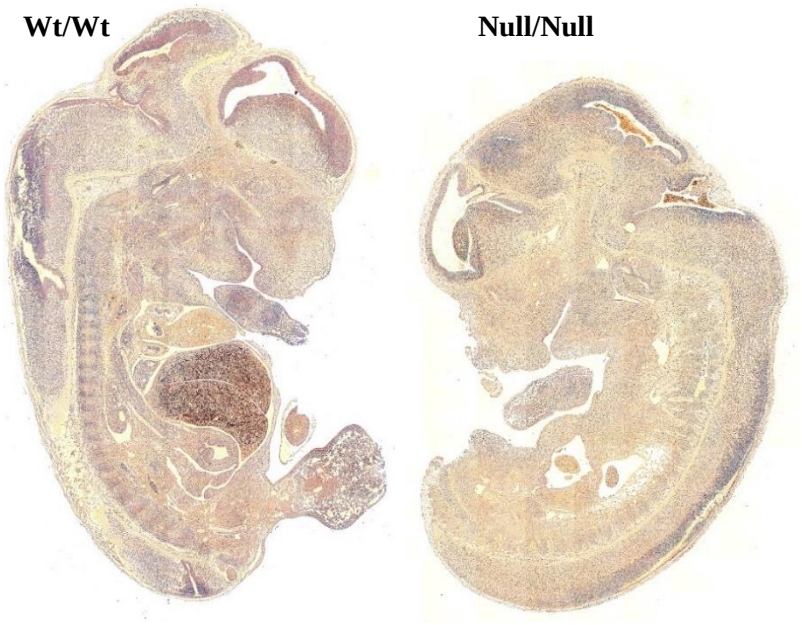
Wt/Wt
Null/Null

(C)

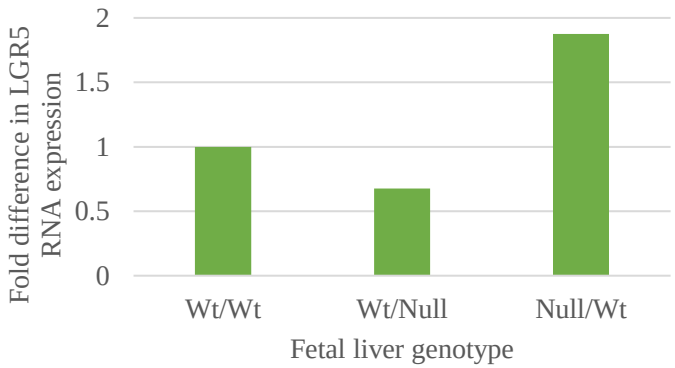
Fold difference in LGR5 RNA expression
2
1.5
1
0.5
0
Wt/Wt
Wt/Null
Null/Wt
Fetal liver genotype

(D)

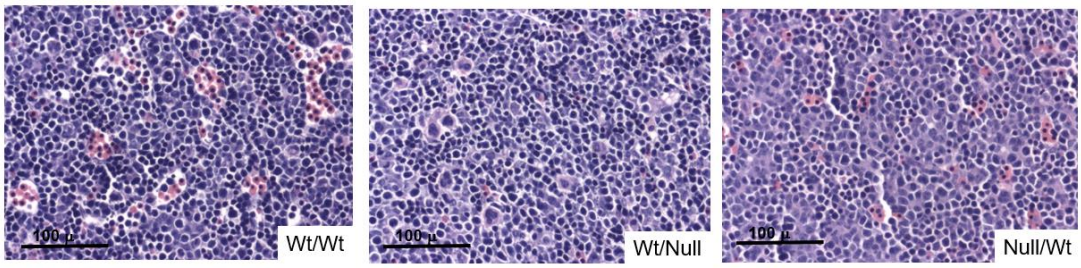

(E)

Age	AGM	Liver
E11.5 (Wt)	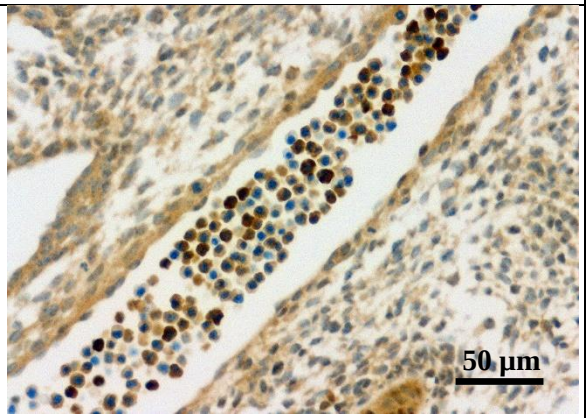	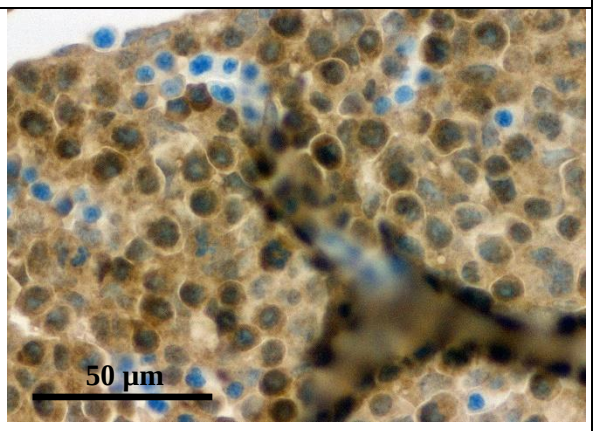
E12.5 (Wt)	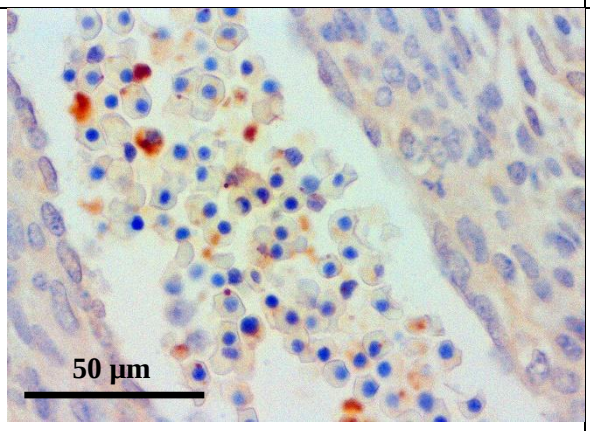	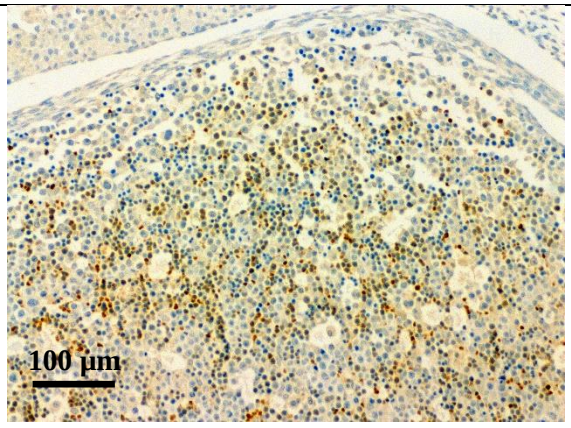

(F)

(G)

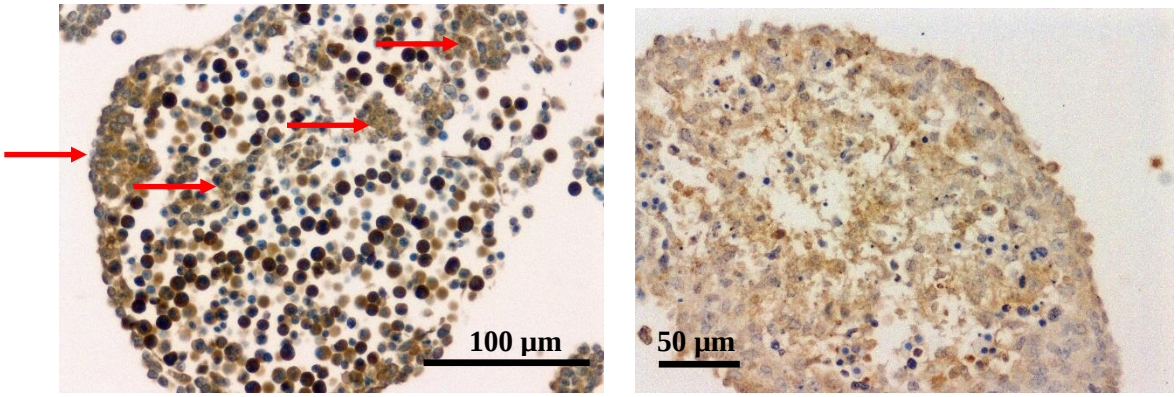

(H)

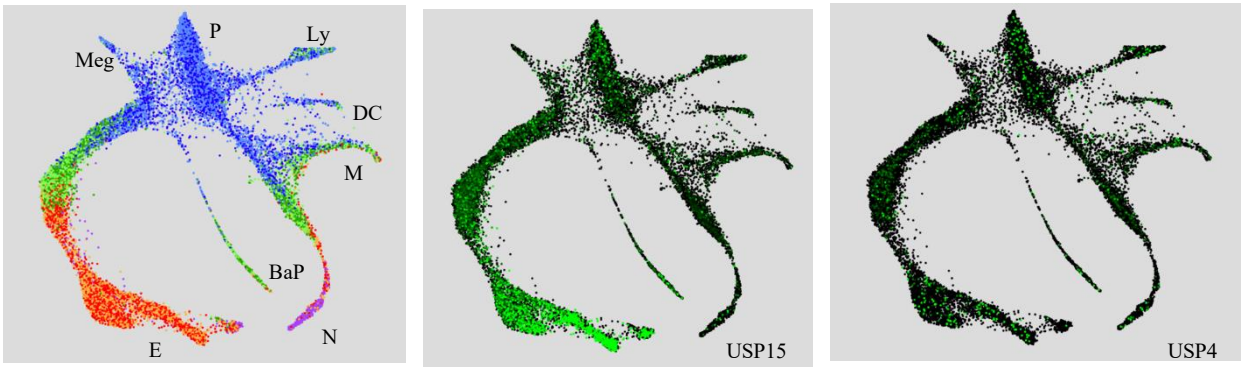

3.5 The stimulated Wnt pathway may be disrupted in MEFs deficient in USP4 and/or USP15

From the results of the growth curve experiment (Figure 4A), it is clear that differences in growth rates are seen in MEFs of different genotypes. This evidence, in combination with the phenotypic differences seen in the embryos and the lethality phenotype, is sufficient to suggest that cellular signalling pathways and substrates are impacted during USP4 and/or USP15 deficiency. As USP4 and USP15 have many substrates in multiple different signalling cascades (12), there are many targets that may explain the phenotype. The Wnt/β-catenin pathway was chosen as a starting point because of its role in lung adenocarcinoma metastasis in USP4 knockdowns (51). Furthermore, this pathway is heavily involved in the fetal hematopoiesis, a process that may be affected in USP deficiency (50). Specifically, the canonical pathway component Wnt3a is particularly important in the fetal liver stage of hematopoiesis, and knockouts of this ligand result in a lethal phenotype by E12.5 in mice (56).

USP4 has more substrates in the Wnt-stimulated pathway, while USP15 has more substrates in the unstimulated pathway. Each DUB differs in the specific substrates that they deubiquitinate- while USP4 deubiquitinates β-catenin, USP15 deubiquitinates APC (24, 33). To interrogate this pathway, not only direct USP4/15 substrates will be analyzed, but also downstream effectors of the pathway such as Zeb1, TCF4 and LGR5 (24, 51, 58). The expression of each of these Wnt target genes are known to be impacted by Wnt stimulation, and thus should be good indicators of Wnt pathway function.

Protein lysates from unstimulated and stimulated cells were produced to investigate both pathways. Due to its purported role in fetal hematopoiesis, the ligand Wnt3a was chosen to stimulate the Wnt pathway to produce stimulated cells (56). Optimization experiments were

carried out by the analysis of β-catenin expression by western blot in the NIH3T3 MEF cell line in order to determine the optimal concentration of Wnt3a ligand and harvesting time after stimulation, either 24h or 48h. By densitometric analysis, expression of β-catenin was normalized to expression of β-actin, a commonly used housekeeping protein in western blotting. The expression of β-catenin is presented relative to the expression of β-catenin at 0 ng/mL of Wnt3a. It was determined that Wnt3a stimulation would be done with 100 ng/mL of Wnt3a and cells would be harvested after 24 h, since expression of β-catenin was optimal at that time and concentration (Figure 8A).

Protein lysates of primary MEFs of each of the following genotypes were produced with or without Wnt3a stimulation: Het/Het, Null/Null, Null/Het, Het/Null, Wt/Wt. The following pathway components were analyzed: β-catenin, the important intracellular signal mediator, Zeb1, the downstream effector that is a direct target gene of β-catenin, TCF4, another downstream effector (and direct USP4 substrate), and APC, a member of the β-catenin degradation complex in the unstimulated Wnt pathway (24, 33, 51). From the raw western blots, it can be seen that expression of β-catenin and Zeb1 are decreased in the Wnt stimulated cells in each genotype (except the reference Wt/Wt, where it increased) (Figure 8B). Figures 8C and 8D confirm this trend by densitometric analysis. In these graphs, expression of each target was normalized to total protein, as described, with the β-actin normalizer protein present in Figure 8B for visual reference. This may indicate that the pathway is unaffected by the loss of allele(s) of USP4 and/or USP15 at rest, but when stimulated, it is affected. This trend is not seen in TCF4 (Figure 8B), a finding that was confirmed by densitometric analysis.

Interestingly, APC, a member of the β-catenin degradation complex and a USP15 substrate (33), was only expressed in the unstimulated (0 ng/mL of Wnt3a) Wt/Wt MEFs (Figure 8E). The

figure also shows the total loaded protein as a normalizer, and to confirm that the lack of expression of APC in the other genotypes is not due to improper loading.

Figure 8. Stimulated canonical Wnt pathway may be impacted by USP4/USP15 deficiency. **(A)** Expression of β-catenin in the 3T3 cell line at indicated concentrations of Wnt3a ligand, harvested 24 hours post-stimulation (green) and 48 hours post-stimulation (blue), was investigated by western blot. Expression is normalized to β-actin and relative to expression of β-catenin at 0 ng/mL of Wnt3a. Densitometrical analysis done on ImageLab software. **(B)** Primary MEFs of each indicated genotype were prepared with or without 100 ng/mL of Wnt3a ligand and expression of β-catenin, Zeb1 and TCF4 were investigated by western blot (n=1). Expression of β-actin and total loaded protein are present as normalizers. **(C)** Densitometric analysis of β-catenin expression in primary MEFs of each indicated genotype with or without 100 ng/mL of Wnt3a ligand. Expression was normalized to total loaded protein and Wt/Wt reference sample. Densitometric analysis was done on ImageLab software. **(D)** Densitometric analysis of Zeb1 expression in primary MEFs of each indicated genotype with or without 100 ng/mL of Wnt3a ligand. Expression was normalized to total loaded protein and Wt/Wt reference sample. Densitometric analysis was done on ImageLab software. **(E)** Expression of APC in the unstimulated primary MEFs of each genotype by western blot. Total loaded protein is also shown as a normalizer.

(A)

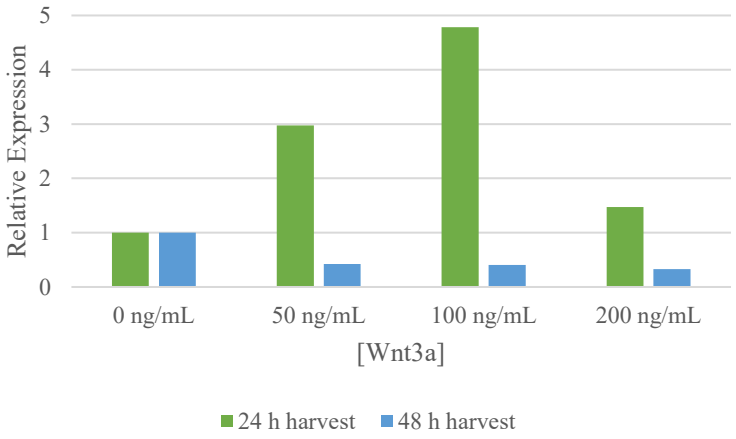
Relative Expression
5
4
3
2
1
0
0 ng/mL
50 ng/mL
100 ng/mL
200 ng/mL
[Wnt3a]
24 h harvest
48 h harvest

(B)

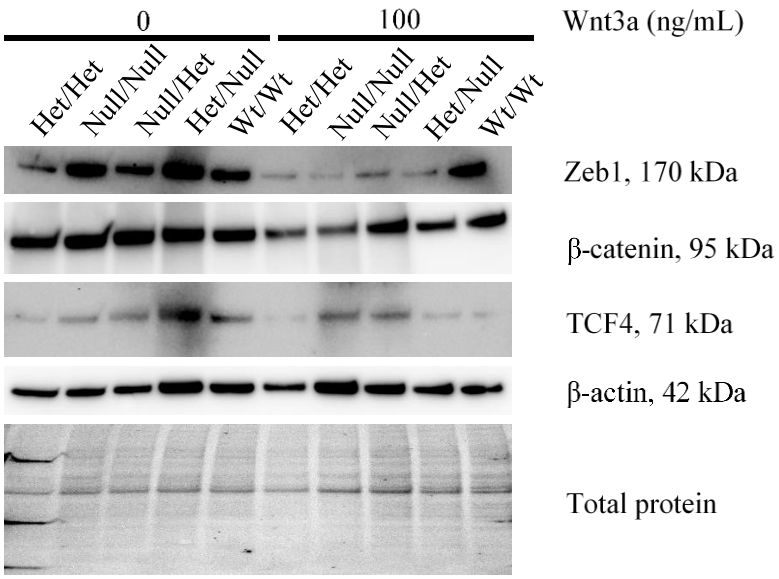
0
100
Wnt3a (ng/mL)
Het/Het
Null/Null
Null/Het
Het/Null
Wt/Wt
Het/Het
Null/Null
Null/Het
Het/Null
Wt/Wt
Zeb1, 170 kDa
β-catenin, 95 kDa
TCF4, 71 kDa
β-actin, 42 kDa
Total protein

(C)

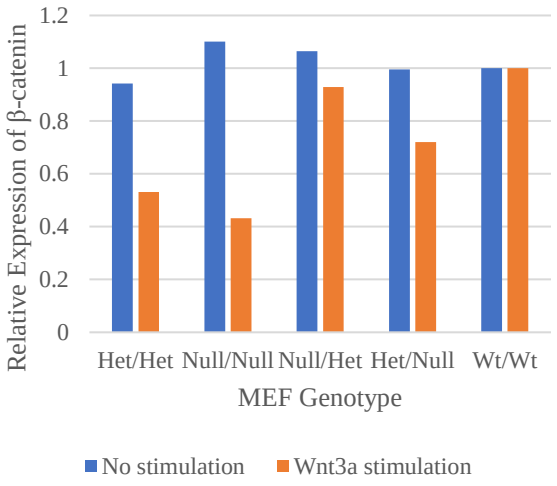
Relative Expression of β-catenin
1.2
1
0.8
0.6
0.4
0.2
0
Het/Het
Null/Null
Null/Het
Het/Null
Wt/Wt
MEF Genotype
No stimulation
Wnt3a stimulation

(D)

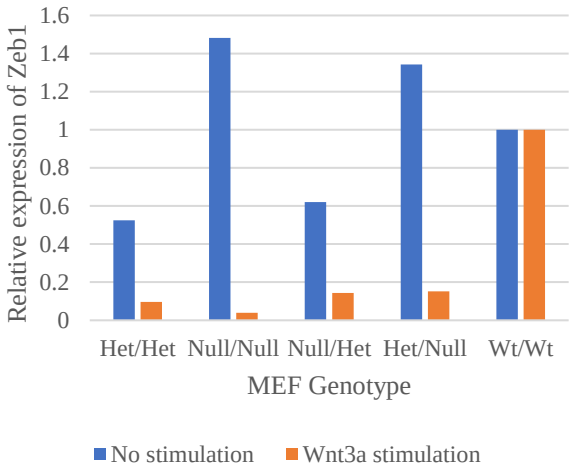
Relative expression of Zeb1
1.6
1.4
1.2
1
0.8
0.6
0.4
0.2
0
Het/Het
Null/Null
Null/Het
Het/Null
Wt/Wt
MEF Genotype
No stimulation
Wnt3a stimulation

(E)

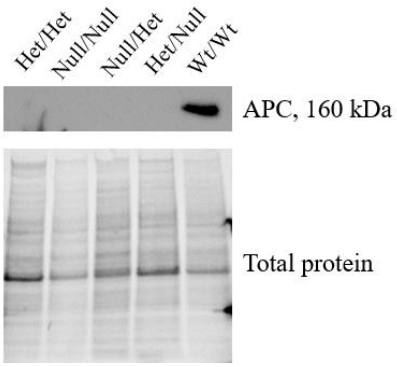
Het/Het
Null/Null
Null/Het
Het/Null
Wt/Wt
APC, 160 kDa
Total protein

3.6 LGR5 is expressed in MEFs and is ubiquitinated

Since LGR5 as a potentially important factor in this system was identified through DNA microarray data in null MEFs, it was important to follow this up with protein and RNA expression studies in MEFs. An antibody for LGR5 was ordered, optimized and validated in positive (mouse ovary) and negative (adult mouse liver) controls (data not shown). Protein lysates of primary MEFs of each of the following genotypes were produced without Wnt3a stimulation: Het/Het, Null/Null, Null/Het, Het/Null, Wt/Wt. By western blot, LGR5 protein expression was analyzed and normalized by total protein (Figure 9A). Interestingly, there is less expression of LGR5 when only one viable allele of one ohnologue is present, but not when both are not present. To dig deeper into this finding, qPCR was conducted on the MEFs with the previously described LGR5 primers. While the RNA expression of LGR5 mirrored the protein presence in Het/Het and Null/Het, there appeared to be less RNA expression than what would be expected given the protein in Null/Null, but more RNA expression than expected for Het/Null (Figure 9B).

The MEFs were also prepared with 100 ng/mL Wnt3a stimulation and a western blot was run. In the stimulated MEF blot, LGR5 appears to have two bands of close molecular weight (Figure 9C). This may be due to a ubiquitinated and de-ubiquitinated LGR5 when the cell is stimulated with Wnt3a. This was further explored using immunoprecipitation to pull down LGR5 from cell lysates, and anti-ubiquitin antibodies to identify the bands. Note that since LGR5 is a membrane protein, it is recommended that the prepared cell lysates are heated at 70 °C for 20 min instead of the usual 95 °C for 5 min seen in normal western blot protocols. As I was unsure how well this antibody would perform in an immunoprecipitation reaction, I performed the immunoprecipitation with the LGR5 antibody on the Wt/Wt cell lysate (either

stimulated with 100 ng/mL Wnt3a or not) and heated one batch of lysates to 70 °C for 20 min and another to 95 °C for 5 min prior to running the gel. The western blot was first probed with an anti-ubiquitin antibody (left panel) and then fully stripped and run with the LGR5 antibody (right panel) (Figure 9D). Both the ubiquitin and LGR5 antibody identified a band at the appropriate molecular weight (approximately 100 kDa). Interestingly, the band appeared in both the Wnt-stimulated (indicated by "100") and unstimulated ("0") lanes. This indicates that in both Wnt-dependent and independent pathways, LGR5 may be ubiquitinated. Although LGR5 is known to modulate Wnt receptors through its interactions with the ubiquitin ligases RNF43 and ZNRF3 (58) the ubiquitination of LGR5 itself has not been previously documented.

Figure 9. LGR5 expression in MEFs. (A) Expression of LGR5 in the unstimulated primary MEFs of each genotype by western blot. Total loaded protein is also shown as a normalizer. **(B)** Quantitative polymerase chain reaction was performed in triplicate on isolated RNA from unstimulated primary MEFs to analyze LGR5 expression at the transcript level. Expression was normalized to PPIA (housekeeping gene) and is shown relative to LGR5 expression in Wt/Wt cells. **(C)** Expression of LGR5 in the stimulated (100 ng/mL of Wnt3a) primary MEFs of each genotype by western blot. Total loaded protein is also shown as a normalizer. Visual inspection and analysis in ImageLab software confirms presence of two bands of close molecular weight in each lane. **(D)** LGR5 antibody was used to pull down protein in Wt/Wt (both unstimulated and stimulated) MEFs in an immunoprecipitation reaction. First two lanes show total cell lysate input prior to immunoprecipitation. Following three lanes show the immunoprecipitated protein lysates that were heated at 70 °C for 20 min prior to gel loading. Final three lanes show the immunoprecipitated protein lysates that were heated at 95 °C for 5 min prior to gel loading. In each of the immunoprecipitated lanes, the first lane is the Wnt-stimulated cell lysate ("100"), the second lane is the unstimulated cell lysate ("0"), and the final lane is the negative control, where no LGR5 antibody was used during the immunoprecipitation. The left panel shows the blot after the anti-Ub antibody was used, and the right panel shows the blot after the anti-LGR5 antibody was used.

(A)

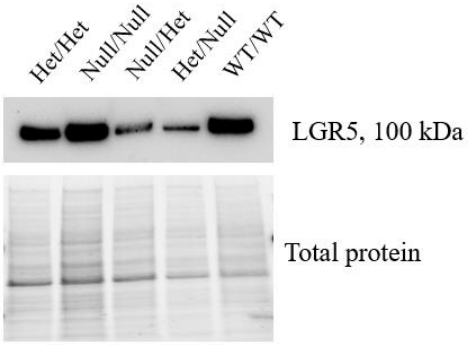
Het/Het
Null/Null
Null/Het
Het/Null
WT/WT
LGR5, 100 kDa
Total protein

(B)

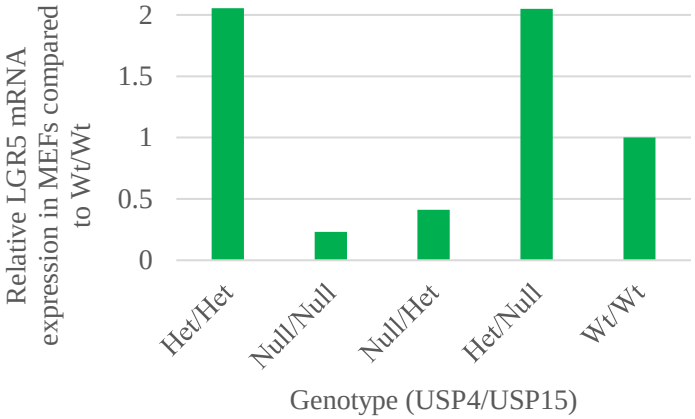
Relative LGR5 mRNA expression in MEFs compared to Wt/Wt
2
1.5
1
0.5
0
Het/Het
Null/Null
Null/Het
Het/Null
Wt/Wt
Genotype (USP4/USP15)

(C)

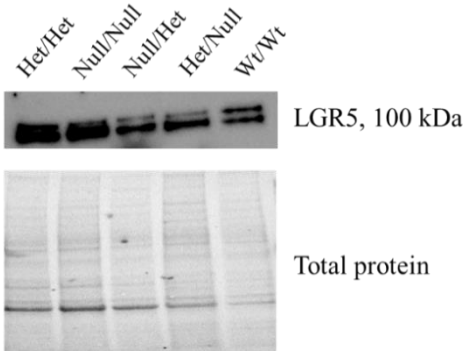
Het/Het
Null/Null
Null/Het
Het/Null
Wt/Wt
LGR5, 100 kDa
Total protein

(D)

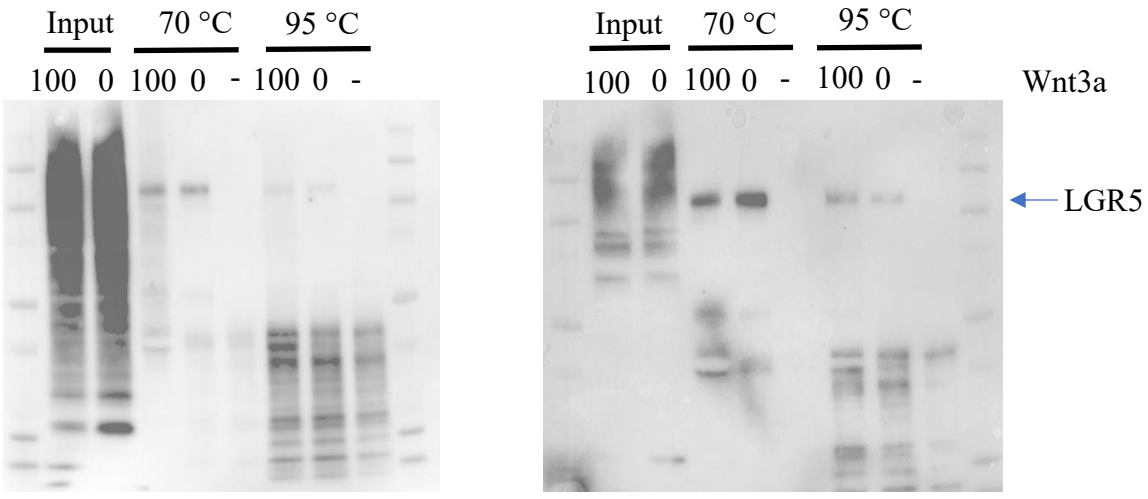
Input
70 °C
95 °C
100 0 100 0 - 100 0 -
Input
70 °C
95 °C
100 0 100 0 - 100 0 -
Wnt3a
LGR5
Anti-Ub
Anti-LGR5

3.7 Transcriptional compensation may explain lack of severe phenotype in mice null for only one ohnologue.

There is evidence of protein functional redundancy in humans and other species, such as in actin-binding proteins (46). Therefore, it is possible that the lack of obvious phenotype seen in mice homozygous null for either USP4 or USP15 may be due to plasticity in the function of the protein or protein feedback loops. To investigate this possibility, we first looked at protein levels of USP4. Densitometric analysis of a western blot demonstrated the expected reduction of USP4 protein expression in null genotypes, and half the amount of expression in heterozygous genotypes, compared to wildtype (Figure 10). This confirms that any functional redundancy is not due to a protein feedback loop that results in increased USP4 protein levels. Despite the abundance of USP15 antibodies commercially available, we have yet to find a specific antibody that does not cross-react with USP4, so we were unable to do the same experiment for USP15.

While there may not be a protein feedback loop at play in this system, there is also evidence that genetic robustness as a product of transcriptional adaptation may allow for functional redundancy. In this mechanism, related genes are upregulated when harmful mutations are present. Recently, a mechanism of genetic compensation called nonsense-induced transcriptional compensation (NITC) was described. In this process, a mutant allele is transcribed to make a mutant mRNA that undergoes degradation. The fragments from degradation can bind DNA of sequences of highly similar genes, causing their upregulation (48). We recently published a paper in the journal *Bioessays*, in which we suggested that USP ohnologues would be good candidates for analysis for this mechanism (42).

To investigate potential transcriptional compensation, RT-qPCR was used as a preliminary analysis. The primers generated for USP4, USP15 and PPIA were used, as previously described. The ΔΔCt method was employed to analyze the data and each sample was compared to a

reference sample of Wt/Wt RNA. Each value in Table 7 is RQ, or relative quantification, meaning it is the fold difference in transcript expression, normalized to the endogenous control (PPIA) and in reference to expression of that transcript in Wt/Wt liver sample. Since the most obvious phenotype was a liver phenotype, the livers from mice of various genotypes were isolated and RNA extracted for the RT-qPCR. As previously mentioned, since we were unable to isolate an intact liver from the Null/Null embryos, we used RNA from the whole embryo for this analysis. As expected, there were negligible USP4 and/or USP15 transcripts detected in the Null/Null genotype. There appeared to be more USP4 expressed in the Het/Null genotype than USP15 expressed in the Null/Het genotype, but both levels were low compared to Wt/Wt. Interestingly, when the USP4 ohnologue was null and the USP15 was Wt (Null/Wt), there is a 7-fold increase in expression of the Wt ohnologue. When the USP15 ohnologue was null and the USP4 was Wt (Wt/Null), there was a 78-fold increase in expression of the Wt ohnologue.

Figure 10. Evidence of transcriptional compensation. By western blot analysis, USP4 protein levels were analyzed in each MEF genotype (Wt/Wt, Het/Het, Null/Null, Null/Het, Het/Null). Expression was normalized by total loaded protein, then compared to Wt/Wt expression to get relative expression levels. Densitometric analysis was done in ImageLab software.

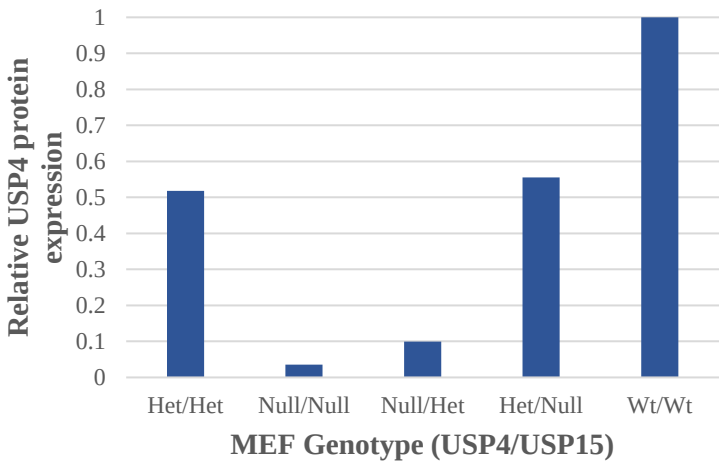
Relative USP4 protein expression
1
0.9
0.8
0.7
0.6
0.5
0.4
0.3
0.2
0.1
0
Het/Het
Null/Null
Null/Het
Het/Null
Wt/Wt
MEF Genotype (USP4/USP15)

Table 7. Relative quantification (RQ) of USP4/USP15.

	USP4	**USP15**
Genotype	RQ	RQ
Wt/Wt liver	1	1
Null/Null MEFs	3.34E-05	1.46E-05
Null/Het liver	0.000687	0.0773
Het/Null liver	0.745	2.98E-05
Null/WT liver	0.0897	7.771
WT/Null liver	78.300	0.764

Relative quantification, or fold change, of USP4 and USP15 transcript expression compared to Wt/Wt in various liver and MEF samples, by RT-qPCR.

CHAPTER 4: DISCUSSION

4.1 Investigation of functional redundancy

After an extensive phylogenetic analysis of USP4 and USP15 across the animal kingdom and over evolutionary time, it was seen that all species contain one or both members of the ohnologue pair (12). It appeared that while USP11, which arose from a small segmental duplication of USP4 in the Devonian geological era, was largely dispensable, USP4 and/or USP15 were not (12). Initial studies in our lab to assess the essentiality of these genes involved acquiring mouse strains with inactivating mutations such that no functional gene product was produced. Both the USP4-null strain and the USP15-null strain appeared viable with no obvious phenotypic effects, which lead us to the conclusion that USP4 and USP15 were functionally redundant. Further evidence was provided when genetic crosses between mice heterozygous for both genes were performed, and progeny of all expected genotypes were produced, with the exception of the compound null (Null in USP4 and Null in USP15). This meant that USP4 and USP15 had enough functional redundancy to rescue the other when inactivating mutations were present. Furthermore, at least one viable allele of this ohnologue pair was needed for viability ($p = 0.000022$) (12).

In order to have a more in-depth Mendelian analysis, each mouse strain was backcrossed to C57BL/6J mice for 10 generations in order to ensure a uniform genetic background. After the same heterozygous crosses were performed ($USP4^{Het}xUSP15^{Het}$), the compound null genotype remained lethal with a high degree of confidence by binomial analysis ($p = (15/16)^{137} = 0.000144$). While we knew that no viable pups were born with the Null/Null genotype, we did not know at what point in embryonic development these Null/Null embryos died. After careful analysis of the embryo litters at various days in development, it was seen that Null/Null embryos

were no longer alive after approximately embryonic day 12.5 (Coulombe, Zachariah, Gray, unpublished). In this study, fertilized zygotes were followed to the blastocyst stage, and all genotypes were present. This finding led us to the logical conclusion that USP4 and USP15 may not be essential in early embryonic development, but rather they may be essential for a particular process that occurs around E12.5. Another possibility is that the lack of USP4 and USP15 leads to errors in some developmental process(es) that accumulate until death at E12.5.

To investigate these possibilities and the ohnologues' functionality at the cellular level, we cultured MEFs from embryos isolated at E12.5 of various genotypes. A growth curve experiment was carried out to determine if any obvious phenotypic differences could be seen between MEFs of various genotypes. As expected, the Null/Null MEFs had the lowest growth rate (Figure 4A). While the MEFs with the highest growth rate (Null/Het genotype) increased by 48-fold during the culture period, Null/Null MEFs only increased by 12-fold. These slow-growing cells made it difficult to passage and to eventually immortalize. While each other MEF genotype was immortalized as described in Chapter 2, the Null/Null MEFs died off too quickly for this same process to be replicated. For this reason, Null/Null MEFs of an early passage number were left in a flask in a 37 °C incubator at 20% O_2 for weeks prior to re-passaging. For this reason, it was not included in Figure 4B.

Taken together, the mouse and MEF data for the Null/Null genotype indicate that the lack of viable USP4 and USP15 alleles results in death of the embryo at approximately E12.5 and MEFs that are slow growing. These observations provide more evidence to the Vlasschaert *et al.* (2015) claim that by phylogenetic analysis, USP11 is largely dispensable and is not functionally redundant with its paralogues, as USP11 is unable to rescue this lethal phenotype (12).

While we have determined that USP11 must not be able to perform the functions of USP4 and USP15, what about the opposite? From a recent article on PTEN self-regulation through USP11, the authors knocked out USP11 in mice using a gene-targeting cassette. They observed that the null mice were viable and progeny were in accordance with Mendelian frequencies (66). The lack of phenotype may indicate that another USP may be able to perform the specific functions of USP11 when deficient, and the likely candidate is USP4, from which USP11 arose. A possible future experiment to test such a hypothesis could be to cross USP4-null mice with USP11-null mice to further explore their relationship and the impact of a SSD versus WGD.

When looking beyond the Null/Null genotype, some interesting observations can be made when comparing the Mendelian ratios of the $USP4^{Het}$x$USP15^{Het}$ cross and the MEF growth curve (Table 4 and Figure 4A, respectively). Firstly, when USP4 is null, there are a higher than expected number of pups born with that genotype. For example, the expected Mendelian ratio of pups born with the Null/Het genotype is 12.5%, however we see 20% with this genotype. In the MEF growth curve, we see that Null/Het MEFs have the highest growth rate, even higher than Het/Het MEFs. This parallel between the mouse and MEF data could indicate that the lack of USP4 may confer a selective advantage. While this surprising conclusion is inevitable given the mouse and MEF data, one must not forget that these are highly artificial conditions. It is possible that the lack of USP4 may remove restraints imposed by USP4-implicated pathways such as p53, innate immunity or DNA repair (27, 28, 67). This could promote proliferation despite increased mutations or susceptibility to viral infections. For example, in an unpublished study, we know that USP4 deficiency leads to enhanced viral replication and compromised innate immunity (Coulombe and Gray, unpublished). In our sterile cell culture conditions and mouse facility,

these deleterious effects would be masked. Therefore, the positive selection we see in our conditions may actually be negative in nature. One way to test this idea may be to challenge our USP4-null mice with viral infection and see how they fare compared with mice of other genotypes. To look for deleterious effects from errors in DNA repair, we should look for an increase in DNA repair foci by staining tissues for gamma-H2AX or 53BP1.

A second observation from the mouse intercross data and MEF growth curve is that when USP15 is null, there are a lower than expected number of pups born with that genotype. For instance, the expected Mendelian ratio of pups of the Het/Null genotype is 12.5%, however we only see 2% with this genotype. Furthermore, in the MEF growth curve, Het/Null MEFs have the second lowest growth rate, only above Null/Null. Taken together, this may indicate that the USP15-null genotype may be diminished in both the mouse and MEF data. According to the aforementioned phylogenetic analysis, USP15 is the most similar ohnologue to the ancestral gene in terms of sequence. This may explain why the loss of USP15 appears to be more impactful than the loss of USP4.

While initial published evidence that only one allele was necessary for viability led to the claim of functional redundancy, the evidence presented here leads to some doubt in this claim. The skewed Mendelian ratios and MEF growth curve data indicate that while there may be partial functional redundancy, USP4 and USP15 cannot perform each other's functions completely.

While other groups have studied USP4 and USP15 separately with respect to various cellular processes and diseases such as cancer, one such study that was recently published in BioRxiv was of particular interest. In this study, the authors generated USP15 knockout mice (C57BL/6J strain) by a CRISPR/Cas9 germline deletion of the entire USP15 locus (68). They

observed interesting phenotypes such as decreased lifespan, decreased body weight and skewed Mendelian transmission in the USP15-null population. These observations made us wonder if our USP15 mouse line developed during the C57BL/J backcrosses had similar phenotypes. We performed a retrospective analysis based on some weight and genotype data that were collected at the time (Figures 5B-E). Firstly, the Mendelian ratios were quite skewed, with 63% of the progeny being USP15-het and only 13% being USP15-null. This is consistent with the aforementioned diminished phenotype we were seeing in the $USP4^{Het}$x$USP15^{Het}$ crosses for Het/Null mice and MEF data. Second, USP15-null mice appear to have decreased body weight compared to their wildtype and heterozygous counterparts, particularly amongst the male mice. A cohort of male mice who were weighed at 5, 6, 7, and 9 weeks show a significant body weight decrease in the null population (Figure 5C). Female USP15-null mice, however, appear to catch up to their heterozygous counterparts, in terms of weight (Figure 5E). A more extensive analysis of these mice must be completed in future experiments to ensure this preliminary retrospective analysis holds true. This can be done by setting up matings, taking tail/ear clippings at birth for genetic analysis and weighing the same cohort of mice every week for the first year of life. This would also allow for more data on survival and length of life depending on genotype. These observations were not seen in a retrospective analysis of our USP4 mouse lines (data not shown). This extensive analysis should take place in the USP15-only strain, USP4-only strain, and in the $USP4^{Het}$x$USP15^{Het}$ genetic crosses.

4.2 Defective hematopoiesis may contribute to Null/Null lethality

USP4 and USP15 have several interacting partners in a variety of cell signaling pathways. Vlasschaert *et al.* (2015) summarizes many of these partners identified by mass proteomic analysis and other independent analyses in Table 2 (12). Because of this wide array of

substrates, there are many possible signaling pathways that may be disrupted in the Null/Null embryos leading to death at embryonic day 12.5. The observations that Null/Null embryos are smaller in size compared to Het/Het counterparts as early as E10.5 and that the Null/Null livers are severely underdeveloped provided us with a starting point for investigating the cause of the lethal phenotype.

The severely underdeveloped liver was of particular interest because hematopoiesis is purported to take place in the liver at the time of Null/Null embryo death. According to the literature, murine hematopoiesis takes place first in the mesoderm (E6.5), yolk sac (E7.5), para-aortic splanchnopleure (E7.5-9.5), AGM (E10.5-11.5), developing fetal liver (E12.5-14.5) and then finally moves to the bone marrow (by E18.5) (55). Furthermore, several fetal hematopoietic defects in the literature, specifically in definitive erythropoiesis, lead to murine embryonic death at the same time point. For example, aberrant expression of the definitive erythropoiesis gene *Fli1* lead to impaired hematopoietic differentiation and death at E12.5 (69). Additionally, deficiency of the RNA-editing enzyme ADAR1 leads to severe defects in definitive hematopoiesis, a disintegrating fetal liver structure, and death between E11.5-12.5 (70). The evidence from the literature point to defective hematopoiesis as a potential explanation for the lethal phenotype observed, and IHC staining with the hematopoietic marker c-kit confirmed it. While the wildtype liver had many hematopoietic cells in various stages of hematopoiesis, the null liver had little to no c-kit staining (data not shown).

Fetal hematopoiesis is a developmental process that requires the coordination of a number of signalling pathways such as TGFβ and canonical Wnt and deficiency in any number of these pathways could be the cause of the hematopoietic defect observed (55). The canonical Wnt pathway components β-catenin and ligand Wnt3a are particularly important during fetal

liver hematopoiesis, and the pathway supports HSC expansion and differentiation (50). When Wnt3a is knocked out, there are many developmental defects and death occurs at E12.5 (56). Due to these important links to hematopoiesis, we took a candidate protein approach to studying the canonical Wnt pathway. Through the stimulated and unstimulated MEFs of various genotypes, we systematically analyzed the following pathway components by western blot: β-catenin, Zeb1, TCF4, APC, and LGR5 (24, 33, 51, 54, 58). Of these candidate proteins, β-catenin, APC and TCF4 are direct USP4/15 substrates and the former two are intracellular mediators of the Wnt signal. The candidate proteins Zeb1, TCF4 and LGR5 are downstream Wnt target genes.

By western blot and densitometric analysis, the pathway component β-catenin and the downstream effector Zeb1 appear to be impacted in MEFs of various genotypes (all lacking at least one allele of USP4 or USP15) particularly in the cells stimulated by Wnt3a (Figure 8B-D). This may indicate that USP4 and USP15 play a more important role in the stimulated pathway (Figure 3). It is important to note that the unstimulated MEFs will likely still have some Wnt stimulation from Wnt ligands exported by other cells, meaning the "unstimulated" MEFs are really "baseline" Wnt signalling MEFs. By adding exogenous Wnt3a ligand, we are forcing more of the cell's Wnt activity to be in the stimulated pathway. By this reasoning, one may expect components like β-catenin and Zeb1 to be upregulated compared to baseline, however we see the opposite in MEFs with genotypes that lack one or more USP4 or USP15 allele. In general, DUBs often exist in complexes with E3 ubiquitin ligases, which perform the opposite function of a DUB and add ubiquitin moieties to proteins. For example, USP4 is known to form a heterodimeric protein complex with Ro52 (E3 ligase). This complex not only regulates other substrate proteins, but they also ubiquitinate and deubiquitinate each other (71). In this case, the

lack of USP4 allele(s) may mean less of this heterodimeric complex, and more Ro52, which may mean more ubiquitination and thus degradation of target proteins.

APC, a member of the β-catenin degradation complex and a USP15 substrate (33), was only expressed in the unstimulated Wt/Wt MEFs (Figure 8E). This may indicate that the loss of even one allele of USP4 or USP15 affects APC, or perhaps the β-catenin degradation complex. The COP9 signalosome (CSN) is known to associate with USP15 and stabilize APC in the β-catenin degradation complex (33). Thus when USP15 is not present (Null) or has reduced expression (Het), APC cannot be deubiquitinated and is degraded. In the Wnt-stimulated MEFs, no expression was seen at all, even in the Wt/Wt MEFs (data not shown). This makes sense since the β-catenin degradation complex is only necessary when the Wnt pathway is not stimulated by exogenous Wnt ligand binding.

LGR5 was another downstream effector of the canonical Wnt pathway whose expression was analyzed in MEFs. It was chosen because of its appearance in the DNA microarray screen (Table 5). By western blot of the baseline (unstimulated) MEFs, there was less expression of LGR5 when only one viable allele of one ohnologue is present, but not when both are not present (Figure 9A). By qPCR, the RNA expression of LGR5 mirrored the protein presence in Het/Het and Null/Het, while there appeared to be less RNA expression than what would be expected given the protein expression in Null/Null and the opposite for Het/Null (Figure 9B). The fact that I was looking for LGR5 expression in MEFs may explain the discrepancy between the protein and mRNA expression. LGR5 is primarily expressed in the proliferating adult stem cells of the intestine (61), hair follicle (72), and stomach (73). In embryonic development, LGR5 marks short term hematopoietic stem and progenitor cells, primarily from E11.5-E12.5 in the AGM and liver (57). In the isolation of mouse embryos at E12.5 for MEF culturing, the liver was removed

in order that the fibroblasts would culture favourably. For this reason, perhaps MEFs are not a biologically meaningful system for the study of LGR5 expression. The MEF system did, however, allow us to perform the immunoprecipitation experiment that revealed, for the first time, that LGR5 is ubiquitinated (Figure 9D).

For a more biologically meaningful system, we turned to the fetal liver. While we were unable to isolate Null/Null livers due to their lack of structural integrity, we were able to isolate livers from other genotypes. By qPCR and IHC, the USP15-null (Wt/Null) livers had less expression of LGR5 than their USP4-null (Null/Wt) counterparts (Figure 7C-D). This observation led us to believe that perhaps the loss of USP15 is more impactful for hematopoiesis than the loss of USP4. Using a tool prepared by a group that provides a single cell RNA map (SPRING plot) of human hematopoietic progenitors, we saw that USP15 was expressed more than USP4 in these progenitors (Figure 7H) (65). In IHC staining of sagittal sections of whole embryos in paraffin, the high expression of LGR5 in the wildtype fetal liver at E11.5-E12.5 and the lack of expression in the null fetal liver is very apparent (Figure 7B, F). Furthermore, there is a decrease in the LGR5+ cells present in the AGM from E11.5 to E12.5, indicating the movement of the primary location of hematopoiesis from AGM to liver (Figure 7E). Overall, this makes LGR5 a good marker of fetal hematopoiesis in our system.

Interestingly, 100% of LGR5-null mice die neonatally due to a gastric distension and a ankyloglossia phenotype, which is the fusion of the tongue to mouth's floor, causing an inability to nurse (74). This may indicate that though LGR5 is a relevant marker of HSCs, the protein itself may not be essential to hematopoiesis. However, that is not to say LGR5 is uninvolved. LGR5's importance to Wnt signalling, and Wnt signalling's importance in hematopoiesis must be further explored. It is known that LGR5 forms a complex with R-spondin that neutralize the

transmembrane E3 ligases Rnf43 and Znrf3 that remove the Wnt Frizzled receptor from the membrane by endocytosis and subsequent lysosomal degradation (58). With less fetal liver expression of LGR5 in some of our systems, perhaps Wnt signaling is diminished by the lack of a LGR5/R-spondin complex to neutralize the E3 ligases. Experiments investigating this specific pathway should shed light on this process. Future experiments should also include using the TopFlash assay to assess Wnt activity in the MEFs and liver cells. Technical difficulties such as isolating Null/Null livers must be overcome to allow for experiments such as culturing liver cells, performing qPCR on the liver to analyze USP4, USP15, and LGR5 levels, and more. Finally, we must also look more into the targets identified by DNA microarray (Table 5 and 6).

In a recent article in the journal BioRxiv that was referenced in chapter 4.1, the reason the authors decided to make a USP15 CRISPR-Cas9 knockout mouse is because they found that it was involved in hematopoiesis. The authors were looking for DUBs that were novel regulators of hematopoietic stem and progenitor cell activity, and used an *in vivo* RNAi screen (68). They found that USP15 shRNAs were highly depleted, and after doing *in vitro* and *in vivo* proliferation studies, they found that USP15 depletion impairs hematopoietic stem and progenitor cells. Surprisingly, they also found that USP4 shRNAs were enriched in their screen, but they did not follow this finding up with in depth studies like they did for USP15. The observation that USP4 shRNAs were enriched may mean that the loss of USP4 has no observable impact on hematopoiesis. This observation, along with our observation that USP4-null livers expressed more LGR5 by qPCR than their wildtype counterparts (Figure 7C), may indicate that the lack of USP4 is actually beneficial to liver hematopoiesis, which may explain the positive selection we see for USP4-null mice in Table 4.

The fact that this group approached the question of DUBs involved in the regulation of hematopoiesis using an unbiased screen and came to the conclusion that USP15 is involved confirms the validity of our findings. This leads to more questions and opportunities for future experiments. One such future experiment should encompass making chimeras with the hematopoietic cells of the bone marrow to assess their function. To do this, bone marrow should be collected from adult mice of various genotypes (wildtype, USP4-null, USP15-null), mixed with wildtype marrow bearing a genetic tag, and transplanted into irradiated mice. The relative survival of the bone marrow of different sources would tell us if there is a difference in the hematopoietic abilities depending on genotype. This can be followed up with the same experiment but using HSCs from the fetal livers of isolated embryos of various genotypes.

One question that remains to be satisfactorily solved is a chicken-or-egg dilemma: what came first, the underdeveloped liver or the hematopoietic defect? What if hematopoiesis was not defective, but simply due to the lack of a supportive microenvironment in the liver, it cannot proceed? In contrast, what if the lack of proper hematopoiesis in the fetal liver leads to its demise? We attempted to solve this problem by looking at compound null embryos prior to E12.5. While we isolated embryos at E10.5 and E11.5, we were only able to get usable sagittal sections from the E11.5. The liver of the e11.5 Null/Null embryo is quite small, has several cells positive for LGR5, but also has some damage. By E12.5, this damage worsens and there are fewer cells positive for LGR5. This may indicate that the HSCs are fine without USP4 or USP15, however it is the lack of a supporting microenvironment in the fetal liver that prevents healthy hematopoiesis from continuing as embryonic development continues to E12.5. The issue with this method is that the liver and hematopoiesis develop simultaneously over time, and thus is it difficult to separate them to understand where the defect lies. This dilemma is very similar to

another group who found that mice null in ADAR1 (adenosine deaminase acting on RNA-1) died between E11.5-E12.5, displayed liver disintegration, and defective definitive hematopoiesis (70). While their study did not reveal a molecular cause for the phenotypes observed explained by ADAR1 deficiency, they did explore this liver and hematopoiesis duality. For example, they performed *in vitro* and *in vivo* (spleen) colony-forming assays with hematopoietic progenitor cells derived from the AGM and fetal liver and found that ADAR1 was essential for the proliferation and survival of these progenitors. Conversely, they also made chimeric mice where null embryonic stem (ES) cell clones were injected into wildtype blastocysts, and the descendants of these ES clones were tracked by PCR. They found that ADAR1-deficient ES cells did not give rise to any cells of the adult liver. These experiments can be carried out in our systems as well in order to better understand this duality and the cause of lethality. Interestingly, mice deficient in the stress-signaling kinase SEK1/MKK4 die at mid-gestation between E10.5-12.5, with severely impaired hepatogenesis and liver formation independent of hematopoiesis (75). Further experiments must be carried out in order to determine if the cause of lethality seen in Null/Null embryos is a hematopoietic defect, a hepatic defect, or a combination.

4.3 Investigating transcriptional compensation in ohnologues

Ohnologues are paralogous genes that arose during a whole genome duplication event, which has only occurred twice in mammalian evolution, called the 2R-WGD hypothesis (9). Ohnologues often have redundant or overlapping functions, making their retention in the genome counterintuitive. Why would an organism expend energy to maintain multiple copies of a gene of similar function in the genome? Many have argued that redundancy is worth the extra energy because it provides a back-up system in case of transmission failure. As we know that the transmission of genetic information during division is an error-prone process, including

redundancy in the message is actually responsible (76). We see evidence for the importance of this back-up system in humans. For example, an analysis human genomes found 13 healthy individuals with disease-causing mutations in 8 genes (44). Another analysis found that genes with highly similar paralogues are three times less likely to have known disease mutations (77).

We can see from the USP4^{Het}xUSP15^{Het} intercrosses described in this thesis that the deletion of only one of these ohnologues results in a mild to undetectable phenotype. In fact, the phenotype was so mild that it required a retrospective analysis in order to figure out that the USP15-null mice were born at a sub-Mendelian frequency and that the male mice were underweight (Figure 5B, C). This observation from our lab led us to do a broader search of USP ohnologues in the literature (42). I did a systematic examination of the literature containing inactivating mutations in USPs in mice and found that in mice with homozygous knockout mutations in USP genes with a conserved ohnologue, the resultant phenotypes were mild to undetectable. For example, *Usp25*$^{-/-}$, which has 65% sequence similarity to its ohnologue *Usp28*, is viable with no growth abnormalities, only an elevated sensitivity to IL-17-dependent inflammation and autoimmunity (78). In another example, *Usp46*$^{-/-}$, which has 92% sequence similarity to its ohnologue *Usp12*, have abnormal circadian rhythm phenotypes and display low immobility in tail suspension and forced swim tests (79). In contrast, in mice with knockout mutations in singleton genes (those without an ohnologue), the resultant phenotype was often lethal or dramatic. For example, the singleton *Usp1*$^{-/-}$ have elevated perinatal lethality due to impaired Fancd2 foci assembly and homologous recombination repair (80). Another singleton, *Usp7*$^{-/-}$ has embryonic lethality between E6.5-7.5, due to stabilization of p53 and cell growth arrest (81).

Now that we have established that this ohnologue rescue is likely not just a phenomenon observed in our USP4/USP15 system, we must find a way to explain such functional redundancy, even if it is partial. A protein feedback loop is an obvious place to begin, however looking at the results of densitometric analysis of a western blot with a USP4 antibody, we see no evidence of upregulation at the protein level (Figure 10). Instead, we see that when mice are heterozygous for USP4, the single allele expresses about half the amount of protein than when USP4 is wildtype. Regardless of the level of USP15 allele presence, when the genotype is Het/Het and Het/Null, we see that USP4 expression is about half that of Wt/Wt, exactly what the genetics would predict, in terms of protein expression.

To look for a mechanism, we must look upstream of protein expression- at transcription. Transcriptional compensation or adaptation is a phenomenon that has been used to explain the disparity in phenotypes seen in model systems using knockdowns versus knockouts. For example, Stainier and colleagues demonstrated that in zebrafish, *vegfaa* (a vascular endothelial growth factor) knockout mutants and knockdown morphants have different resultant phenotypes, and only the knockout mutants show upregulation of the closely related gene *vegfab* (82). A recent article from this group suggested a mechanism for transcriptional compensation that hinges on mutant mRNA degradation (48). The mechanism, called NITC, involves the transcription of a mutant allele containing a premature stop codon, and its subsequent degradation by nonsense-mediated decay. This decay is followed by the upregulation of genes with high sequence similarity to the mutant gene's mRNA. In our system, the mice with inactivated USP4 or USP15 were done in such a way to acquire a premature stop codon, meaning our system meets the requirements for NITC to occur.

To begin a preliminary investigation of such a mechanism, we looked at transcript expression of USP4 and USP15 by RT-qPCR in the following samples: Wt/Wt liver, Null/Null MEFs (no Null/Null liver was able to be isolated successfully), Null/Het liver, Het/Null liver, Null/Wt liver, and Wt/Null liver. The amount of each mRNA transcript was normalized to PPIA, the housekeeping normalizer gene, and then compared to Wt/Wt liver, giving us a RQ value, or the fold difference (Table 7). From these results, the most interesting RQ is seen in the Null/Wt and Wt/Null samples, where the Wt allele in each case has a large fold change. This may demonstrate compensation in an ohnologue USP when the related USP is knocked out. To our knowledge, this is the first evidence of transcriptional compensation in DUBs.

Despite this interesting finding, the question of the disparity between the protein findings (by western blot) and the RNA findings (by RT-qPCR) remains. In Figure 10, we do not see an increase amount of the corresponding ohnologue protein when the other is null, and according to our hypothesis, undergoing NITC. However, we also do not see an obvious phenotypic difference between the mice that are of the genotype Het/Het, Wt/Wt, Null/Het, and Het/Null, presumably meaning that the lacking protein's functions are being completed. In short, how can there be RNA rescue and phenotypic rescue, without protein rescue? More work must be done to answer this question but there are a few possibilities. As previously mentioned, DUBs do not linger in the cell alone, and are often part of complexes or interact with E3 ligases. They are often implicated in feedback loops that can lead to complexities in their homeostasis in the cell. Another possibility is that the western blot is not sensitive enough to capture a marginal increase in protein, and a more sensitive proteomic approach is necessary. Finally, it is possible that NITC induces an increase in protein in only a specific subset of cells, thus total lysate from MEFs cannot capture this. The obvious first place to look is at the fetal liver.

Our preliminary RT-qPCR approach has its limits but opens the door to many future studies. To look specifically for evidence of the NITC mechanism, we must look for mutant mRNA fragments using specific primers. To test if nonsense-mediate decay of mutant mRNA is propelling the observed increase in wildtype ohnologue transcripts, we can use pharmacological inhibitors of nonsense-mediated decay (83) or knock down nonsense-mediated decay factors involved in mRNA surveillance machinery such as UPF1(84). Furthermore, a broader transcriptome analysis by RNA-seq in each genotype should provide interesting information.

4.4 Concluding remarks

The objective of this thesis was to delve into the potential functional redundancy of the ohnologue DUB pair USP4 and USP15. Through various experiments, we demonstrated that USP4 and USP15 may only have partial functional redundancy and the lack of USP15 may produce a more severe phenotype than the lack of USP4. We showed that while the compound null genotype is lethal, compound null embryos survive until E12.5 and have a severely underdeveloped liver. We surmised that the lethal phenotype was likely the result of a hematopoietic defect, though more work must be done to identify if there is a simultaneous and/or separate hepatic defect. Finally, we did some preliminary work on investigating transcriptional compensation and demonstrated the first mammalian evidence of NITC in DUBs.

There are a number of potential implications for this work. The study of the USP4 and USP15 gene ohnologues is the first look into DUB evolution and the consequences of WGD in terms of the rewiring of molecular networks. Furthermore, the study of functional redundancy in this ohnologue system important in the context of cancer therapeutics. USP4 is an attractive therapeutic target in cancer that many groups are attempting to target using inhibitors. Published reports assert a role for USP4 in metastatic spread of lung cancer to the brain, mediated by its

effects on the Wnt/ β-catenin pathway. However, potential functional compensation by USP15 must be evaluated before targeted therapies can be considered. Furthermore, as we have uncovered their links to hematopoiesis, the potential impact of this association must also be taken into consideration. Further studies are needed to follow up on the ideas generated by this work.

CONTRIBUTIONS OF COLLABORATORS

Josée Coulombe of the Gray lab set up the mouse crosses and took tail/ear clippings from pups born for genotyping. She also provided the USP15 strain's weight data used for the retrospective analysis, which was collected prior to my arrival in the lab. Josée assisted me in isolating embryos at various stages as well as fetal livers at E12.5.

Mei Zhang of the Gray lab performed the sectioning of isolated embryos in paraffin and immunohistochemistry using the LGR5 antibody.

DNA microarray experiment was performed prior to my arrival in the lab, by Doug Gray and Josée Coulombe.

The Usp4 and Ppia primers were made by a previous student in the lab.

REFERENCES

1. Kravtsova-ivantsiv, Y., and Ciechanover, A. (2012) Non-canonical ubiquitin-based signals for proteasomal degradation. *Journal of Cell Science*. **125**, 539–548

2. Chen, Z. J., and Sun, L. J. (2009) Nonproteolytic Functions of Ubiquitin in Cell Signaling. *Molecular Cell*. **33**, 275–286

3. Grabbe, C., Husnjak, K., and Dikic, I. (2011) The spatial and temporal organization of ubiquitin networks. *Nat Rev Mol Cell Biol*. **12**, 295–307

4. Li, W., Bengtson, M. H., Ulbrich, A., Matsuda, A., Reddy, V. A., Orth, A., Chanda, S. K., and Batalov, S. (2008) Genome-Wide and Functional Annotation of Human E3 Ubiquitin Ligases Identifies MULAN , a Mitochondrial E3 that Regulates the Organelle's Dynamics and Signaling. *PLoS ONE*. **3**, e1487

5. Harrigan, J. A., Jacq, X., Martin, N. M., and Jackson, S. P. (2018) Deubiquitylating enzymes and drug discovery: emerging opportunities. *Nat Rev Drug Discov*. **17**, 57–78

6. Bergthorsson, U., Andersson, D. I., and Roth, J. R. (2007) Ohno's dilemma : Evolution of new genes under continuous selection. *PNAS*. **104**, 17004–17009

7. Vlasschaert, C., Cook, D., Xia, X., and Gray, D. A. (2017) The Evolution and Functional Diversification of the Deubiquitinating Enzyme Superfamily. *Genome Biol. Evol.* **1**, 1–16

8. International Human Genome Sequencing Consortium (2001) Initial sequencing and analysis of the human genome. *Nature*. **409**, 860–921

9. Ohno, S. (1970) *Evolution by Gene Duplication*, Springer-Verlag

10. Dehal, P., and Boore, J. L. (2005) Two Rounds of Whole Genome Duplication in the Ancestral Vertebrate. *PLoS Biology*. **3**, e314

11. Valero, R., Bayés, M., Sánchez-font, M. F., González-, O., Gonzàlez-duarte, R., and Marfany, G. (2001) Characterization of alternatively spliced products and tissue- specific isoforms of USP28 and USP25. *Genome Biology*. **2**, 0043.1–0043.10

12. Vlasschaert, C., Xia, X., Coulombe, J., and Gray, D. A. (2015) Evolution of the highly networked deubiquitinating enzymes USP4 , USP15 , and USP11. *BMC Evolutionary Biology*. **15**, 1–18

13. Zhang, Z., Yang, H., and Wang, H. (2014) The Histone H2A Deubiquitinase USP16 Interacts with HERC2 and Fine-tunes Cellular Response to DNA Damage. *Journal of Biological Chemistry*. **289**, 32883–32894

14. Gupta, K., Copeand, N. G., Gilbert, D. J., Jenkins, N. A., and Gray, D. A. (1993) Unp , a mouse gene related to the tre oncogene. *Oncogene*. **8**, 2307–2310

15. Frederick, A., Rolfe, M., and Chiu, M. I. (1998) The human UNP locus at 3p21 . 31 encodes two tissue-selective , cytoplasmic isoforms with deubiquitinating activity that have reduced expression in small cell lung carcinoma cell lines. *Oncogene*. **16**, 153–165

16. Soboleva, T. A., Jans, D. A., Johnson-saliba, M., and Baker, R. T. (2005) Nuclear-Cytoplasmic Shuttling of the Oncogenic Mouse UNP / USP4 Deubiquitylating Enzyme. *Journal of Biological Chemistry*. **280**, 745–752

17. Gray, D. A., Inazawa, J., Gupta, K., Wong, A., Ueda, R., and Takahashi, T. (1995) Elevated expression of Unph , a proto-oncogene at 3p21 . 3 , in human lung tumors. *Oncogene*. **10**, 2179–2183

18. Surowiak, P., and Budczies, J. (2013) Online Survival Analysis Software to Assess the Prognostic Value of Biomarkers Using Transcriptomic Data in Non-Small-Cell Lung Cancer. *PLoS ONE*. **8**, e82241

19. Heo, M. J., Kim, Y. M., Koo, J. H., Yang, Y. M., An, J., Lee, K., Lee, S. J., Kim, K. M., Park, J., and Kim, S. G. (2014) microRNA-148a dysregulation discriminates poor prognosis of hepatocellular carcinoma in association with USP4 overexpression. *Oncotarget*. **5**, 2792–2806

20. Zhang, L., Zhou, F., Drabsch, Y., and Snaar-jagalska, E. (2012) USP4 is regulated by Akt phosphorylation and deubiquitylates TGF- β type I receptor. *Nat Cell Biol*. **14**, 717–726

21. Fruscio, M. Di, Gilchrist, C. A., Baker, R. T., and Gray, D. A. (1998) Genomic structure of Unp , a murine gene encoding a ubiquitin-specific protease. *Biochim Biophys Acta*. **398**, 9–17

22. Gilchrist, C. A., Gray, D. A., and Baker, R. T. (1997) A Ubiquitin-specific Protease That Efficiently Cleaves the Ubiquitin-Proline Bond. *Journal of Biological Chemistry*. **272**, 32280–32285

23. Vlasschaert, C., Xia, X., and Gray, D. A. (2016) Selection preserves Ubiquitin Specific Protease 4 alternative exon skipping in therian mammals. *Scientific Reports*. 10.1038/srep20039

24. Zhao, B., Schlesiger, C., Masucci, M. G., and Lindsten, K. (2009) The ubiquitin specific protease 4 (USP4) is a new player in the Wnt signalling pathway. *Journal of Cellular & Molecular Medicine*. **13**, 1886–1895

25. Zhang, X., Berger, F. G., Yang, J., and Lu, X. (2011) USP4 inhibits p53 through deubiquitinating and stabilizing ARF-BP1. *The EMBO Journal*. **30**, 2177–2189

26. Milojevi, T., Reiterer, V., Stefan, E., Korkhov, V. M., Dorostkar, M. M., Ducza, E., Ogris, E., Boehm, S., Freissmuth, M., and Nanoff, C. (2006) The Ubiquitin-Specific Protease Usp4 Regulates the Cell Surface Level of the A2a Receptor. *Molecular Pharmachology*. **69**, 1083–1094

27. Fan, Y., Yu, Y., Mao, R., Tan, X., Xu, G., Zhang, H., Lu, X., Fu, S., and Yang, J. (2011) USP4 targets TAK1 to downregulate TNFa -induced NF- kB activation. *Cell Death and Differentiation*. **18**, 1547–1560

28. Xiao, N., Li, H., Luo, J., Wang, R., Chen, H., Chen, J., and Wang, P. (2012) Ubiquitin-specific protease 4 (USP4) targets TRAF2 and TRAF6 for deubiquitination and inhibits TNFα -induced cancer cell migration. *Biochem. J.* **441**, 979–986

29. Song, E. J., Werner, S. L., Neubauer, J., Stegmeier, F., Aspden, J., Rio, D., Harper, J. W., Elledge, S. J., Kirschner, M. W., and Rape, M. (2010) The Prp19 complex and the Usp4 Sart3 deubiquitinating enzyme control reversible ubiquitination at the spliceosome. *Genes & Development*. **24**, 1434–1447

30. Blanchette, P., Gilchrist, C. A., Baker, R. T., and Gray, D. A. (2001) Association of UNP , a ubiquitin-specific protease , with the pocket proteins pRb , p107 and p130. *Oncogene*. **20**, 5533–5537

31. Baker, R. T., Wang, X., Woollatt, E., White, J. A., and Sutherland, G. R. (1999) Identification , Functional Characterization , and Chromosomal Localization of USP15 , a Novel Human Ubiquitin-Specific Protease Related to the UNP Oncoprotein , and a Systematic Nomenclature for Human Ubiquitin-Specific Proteases. *Genomics*. **59**, 264–274

32. Angelats, C., Wang, X., Jermiin, L. S., Copeland, N. G., Jenkins, N. A., and Baker, R. T. (2003) Isolation and characterization of the mouse ubiquitin-specific protease Usp15. *Mammalian Genome*. **14**, 31–46

33. Huang, X., Langelotz, C., Hetfeld-Pechoc, B. K. J., Schwenk, W., Dubiel, W., and Berlin, U. (2009) The COP9 Signalosome Mediates β -Catenin Degradation by Deneddylation and Blocks Adenomatous Polyposis coli Destruction via USP15. *J. Mol. Biol.* **391**, 691–702

34. Aggarwal, K., Massague, J. (2012) Ubiquitin removal in the TGF-B pathway. *Nature Cell Biology*. **14**, 656–657

35. Eichhorn, P. J. A., Rodón, L., Gonzàlez-juncà, A., Dirac, A., Gili, M., Martínez-sáez, E., Aura, C., Barba, I., Peg, V., Prat, A., Cuartas, I., Jimenez, J., García-dorado, D., Sahuquillo, J., Bernards, R., Baselga, J., and Seoane, J. (2012) USP15 stabilizes TGF- β receptor I and promotes oncogenesis through the activation of TGF- β signaling in glioblastoma. *Nature Medicine*. **18**, 429–436

36. Schweitzer, K., Bozko, P. M., Dubiel, W., and Naumann, M. (2007) CSN controls NF-kB by deubiquitinylation of IkBa. *The EMBO Journal*. **26**, 1532–1541

37. Long, L., Thelen, J. P., Furgason, M., Haj-yahya, M., Brik, A., Cheng, D., Peng, J., and Yao, T. (2014) The U4/U6 recycling factor SART3 has histone chaperone activity and associates with USP15 to regulate H2B deubiquitination. *Journal of Biological Chemistry*. **289**, 8916–8930

38. Zou, Q., Jin, J., Hu, H., Li, H. S., Romano, S., Xiao, Y., Nakaya, M., Zhou, X., Cheng, X., Yang, P., Lozano, G., Zhu, C., Watowich, S. S., Ullrich, S. E., and Sun, S.-C. (2014) USP15 stabilizes MDM2 to mediate cancer cell survival and inhibit antitumor T cell responses. *Nat Immunol.* **15**, 562–570

39. Zhao, B., Velasco, K., Sompallae, R., Pfirrmann, T., Masucci, M., and Lindsten, K. (2012) The ubiquitin specific protease-4 (USP4) interacts with the S9/Rpn6 subunit of the proteasome. *Biochemical and Biophysical Research Communications*. **427**, 490–496

40. Zimmermann, P., Hennig, L., and Gruissem, W. (2005) Gene-expression analysis and

network discovery using Genevestigator. *Trends in Plant Science*. **10**, 407–409

41. Okada, K., Qi, Y., Taniguchi, K., Yoshida, A., Akiyama, T., Yoshioka, Y., Onose, J., Koshino, H., Takahashi, S., and Yajima, A. (2013) Vialinin A is a ubiquitin-specific peptidase inhibitor. *Bioorganic & Medicinal Chemistry Letters*. **23**, 4328–4331

42. Zachariah, S., and Gray, D. A. (2019) Deubiquitinating Enzymes in Model Systems and Therapy : Redundancy and Compensation Have Implications. *BioEssays : news and reviews in molecular, cellular and developmental biology*. 10.1002/bies.201900112

43. El-brolosy, M. A., and Stainier, D. Y. R. (2017) Genetic compensation : A phenomenon in search of mechanisms. *PLoS Genetics*. **13**, e1006780

44. Chen, R., Shi, L., Hakenberg, J., Naughton, B., Sklar, P., Zhang, J., Zhou, H., Tian, L., Prakash, O., Lemire, M., Sleiman, P., Cheng, W., Chen, W., Shah, H., Shen, Y., Fromer, M., Omberg, L., Deardorff, M. A., Zackai, E., Bobe, J. R., Levin, E., Hudson, T. J., Groop, L., Wang, J., Hakonarson, H., Wojcicki, A., Diaz, G. A., Edelmann, L., Schadt, E. E., and Friend, S. H. (2016) Analysis of 589 , 306 genomes identifies individuals resilient to severe Mendelian childhood diseases. *Nature Biotechnology*. **34**, 531–538

45. Nowak, M. A., Boerlijst, M. C., Cooke, J., and Smith, J. M. (1997) Evolution of genetic redundancy. *Letters to Nature*. **388**, 167–171

46. Mills, M. A., Yang, N., Weinberger, R. P., Woude, D. L. Vander, Beggs, A. H., Easteal, S., and North, K. N. (2001) Differential expression of the actin-binding proteins , α -actinin-2 and -3 , in different species : implications for the evolution of functional redundancy. *Human Molecular Genetics*. **10**, 1335–1346

47. O'Leary, M. N., Schreiber, K. H., Zhang, Y., Hale, S., Academia, E. C., Shah, S. R., Morton, J. F., Holstein, C. A., Martin, D. B., Kaeberlein, M., Ladiges, W. C., Fink, P. J., Mackay, V. L., Wiest, D. L., and Kennedy, B. K. (2013) The Ribosomal Protein Rpl22 Controls Ribosome Composition by Directly Repressing Expression of Its Own Paralog, Rpl22l1. *PLoS Genetics*. **9**, e1003708

48. El-brolosy, M. A., Kontarakis, Z., Rossi, A., Kuenne, C., Günther, S., Fukuda, N., Kikhi, K., Boezio, G. L. M., Takacs, C. M., Lai, S., Fukuda, R., Gerri, C., Giraldez, A. J., and Stainier, D. Y. R. (2019) Genetic compensation triggered by mutant mRNA degradation. *Nature*. **568**, 193–197

49. Clevers, H. (2006) Wnt / β -Catenin Signaling in Development and Disease. *Cell*. **127**, 469–480

50. Richter, J., Traver, D., Willert, K., and Jolla, L. (2017) The role of Wnt signaling in hematopoietic stem cell development. *Critical Reviews in Biochemistry and Molecular Biology*. **52**, 414–424

51. Hwang, S. J., Lee, H. W., Kim, H. R., Lee, H., Shin, C. H., Yun, S., Lee, D. H., Kim, D., Kim, K. K., Joo, K. M., and Kim, H. H. (2016) Ubiquitin-specific protease 4 controls metastatic potential through β -catenin stabilization in brain metastatic lung adenocarcinoma. *Scientific Reports*. **6**, 21596

52. Stewart, D. J. (2014) Wnt Signaling Pathway in Non – Small Cell Lung Cancer. *Journal*

of the National Cancer Institute. **106**, djt365

53. Gonzalez, D. M., and Medici, D. (2015) Signaling mechanisms of the epithelial-mesenchymal transition. *Science Signaling*. **7**, re8

54. Luo, K. (2016) Signaling Cross Talk between TGF- b / Smad and Other Signaling Pathways. *Cold Spring Harbour Perspectives in Biology*. **9**, a022137

55. Baron, M. H., Isern, J., and Fraser, S. T. (2012) The Embryonic Origins of Erythropoiesis in Mammals. *Blood*. 10.1182/blood-2012-01-153486

56. Luis, T. C., Naber, B. A. E., Fibbe, W. E., van Dongen, J. J. M., and Staal, F. J. T. (2010) Wnt3a nonredundantly controls hematopoietic stem cell function and its deficiency results in complete absence of canonical Wnt signaling. *Blood*. **116**, 496–497

57. Liu, D., He, X. C., Qian, P., Barker, N., Trainor, P. A., Clevers, H., Liu, H., and Li, L. (2014) Leucine-rich Repeat-containing G-protein-coupled Receptor 5 Marks Short-term Hematopoietic Stem and Progenitor Cells during Mouse Embryonic Development. *Journal of Biological Chemistry*. **289**, 23809–23816

58. Lau, W. De, Peng, W. C., Gros, P., and Clevers, H. (2014) The R-spondin / Lgr5 / Rnf43 module : regulator of Wnt signal strength. *Genes & Development*. **28**, 305–316

59. Zhang, X., Xu, M., Su, S., Zhou, Z., Yang, H., and Zhao, S. (2016) Lgr5-positive cells in the lung and their clinical significance in patients with lung adenocarcinoma. *Molecular and Clinical Oncology*. **5**, 283–288

60. Xu, J. (2005) Preparation, Culture, and Immortalization of Mouse Embryonic Fibroblasts. *Current Protocols in Molecular Biology*. 10.1002/0471142727.mb2801s70

61. Munoz, J., Stange, D. E., Schepers, A. G., De, M. Van, Koo, B., Itzkovitz, S., Volckmann, R., Kung, K. S., Koster, J., Radulescu, S., Myant, K., Versteeg, R., Sansom, O. J., Es, J. H. Van, Barker, N., Oudenaarden, A. Van, Mohammed, S., Heck, J. R., and Clevers, H. (2012) The LGR5 intestinal stem cell signature: robust expression of proposed quiescent ' + 4 ' cell markers. *EMBO Journal*. 10.1038/emboj.2012.166

62. Feng, A., He, Y., Liu, X., Li, J., and Tu, Y. (2014) Expression of USP15, TβR- I and Smad7 in Psoriasis. *Journal of Huazhong University of Science and Technology [Medical Sciences]*. **34**, 415–419

63. Parrinello, S., Samper, E., Krtolica, A., Goldstein, J., Melov, S., and Campisi, J. (2003) Oxygen sensitivity severely limits the replicative lifespan of murine fibroblasts. *Nature Cell Biology*. **5**, 741–747

64. Feroze-Merzoug, F., Berquin, I. M., Dey, J., and Chen, Y. Q. (2002) Peptidylprolyl Isomerase A (PPIA) as a Preferred Internal Control Over GAPDH and β-Actin in Quantitative RNA Analyses. *BioTechniques*. **32**, 776–782

65. Pellin, D., Loper, M., Baricordi, C., Wolock, S. L., Weinberg, O. K., Bif, A., Klein, A. M., Biasco, L., and Montepeloso, A. (2019) A comprehensive single cell transcriptional landscape of human hematopoietic progenitors. *Nature Communications*. **10**, 2395

66. Park, M. K., Yao, Y., Xia, W., Setijono, S. R., Kim, J. H., Vila, I. K., Chiu, H., Wu, Y., Billalabeitia, E. G., Lee, M. G., Kalb, R. G., Hung, M., Paolo, P., Song, S. J., and Song, M. S. (2019) PTEN self-regulates through USP11 via the PI3K- FOXO pathway to stabilize tumor suppression. *Nature Communications*. **10**, 10.1038

67. Zhang, X., Berger, F. G., Yang, J., and Lu, X. (2011) USP4 inhibits p53 through deubiquitinating. *EMBO Journal*. **30**, 2177–2189

68. Van Den Berk, P., Lancini, C., Company, C., and Serresi, M. (2020) USP15 deubiquitinase safeguards hematopoiesis and genome integrity in hematopoietic stem cells and leukemia cells. *BioRxiv*

69. Spyropoulos, D. D., Pharr, P. N., Lavenburg, K. I. M. R., Jackers, P., Papas, T. S., Ogawa, M., and Watson, D. K. (2000) Hemorrhage , Impaired Hematopoiesis , and Lethality in Mouse Embryos Carrying a Targeted Disruption of the Fli1 Transcription Factor. *Molecular and Cellular Biology*. **20**, 5643–5652

70. Hartner, J. C., Schmittwolf, C., Kispert, A., Mu, A. M., Higuchi, M., and Seeburg, P. H. (2004) Liver Disintegration in the Mouse Embryo Caused by Deficiency in the RNA-editing Enzyme ADAR1. *Journal of Biological Chemistry*. **279**, 4894–4902

71. Wada, K., and Kamitani, T. (2006) UnpEL/Usp4 is ubiquitinated by Ro52 and deubiquitinated by itself. *Biochemical and Biophysical Research Communications*. **342**, 253–258

72. Chai, R., Xia, A., Wang, T., Jan, T. A., Hayashi, T., Bermingham-McDonogh, O., Cheng, A. (2011) Dynamic Expression of Lgr5 , a Wnt Target Gene, in the Developing and Mature Mouse Cochlea. *Journal of the Association for Research in Otolaryngology*. **12**, 455–469

73. Barker, N., Huch, M., Kujala, P., Wetering, M. Van De, Snippert, H. J., Es, J. H. Van, Sato, T., Stange, D. E., Begthel, H., Born, M. Van Den, Danenberg, E., Brink, S. Van Den, Korving, J., Abo, A., Peters, P. J., Wright, N., Poulsom, R., and Clevers, H. (2010) Lgr5+ve Stem Cells Drive Self-Renewal in the Stomach and Build Long-Lived Gastric Units In Vitro. *Stem Cell*. **6**, 25–36

74. Morita, H., Mazerbourg, S., Bouley, D. M., Luo, C., Kawamura, K., Kuwabara, Y., Baribault, H., Tian, H., and Hsueh, A. J. W. (2004) Neonatal Lethality of LGR5 Null Mice Is Associated with Ankyloglossia and Gastrointestinal Distension. *Molecular and Cellular Biology*. **24**, 9736–9743

75. Nishina, H., Vaz, C., Billia, P., Nghiem, M., Sasaki, T., Luis, J., Pompa, D., Furlonger, K., Paige, C., Hui, C., Fischer, K., Kishimoto, H., Iwatsubo, T., Katada, T., Woodgett, J. R., and Penninger, J. M. (1999) Defective liver formation and liver cell apoptosis in mice lacking the stress signaling kinase SEK1 / MKK4. *Development*. **126**, 505–516

76. Tautz, D. (1992) Redundancies, Development, and the Flow of Information. *BioEssays : news and reviews in molecular, cellular and developmental biology*. **14**, 263–266

77. Hsiao, T., and Vitkup, D. (2008) Role of Duplicate Genes in Robustness against Deleterious Human Mutations. *PLoS Genetics*. **4**, e1000014

78. Zhong, B., Liu, X., Wang, X., Chang, S. H., Liu, X., Wang, A., Joseph, M., and Dong, C. (2013) Negative regulation of IL-17-mediated signaling and inflammation by ubiquitin-specific protease 25. *Nature Immunology*. **13**, 1110–1117

79. Tomida, S., Mamiya, T., Sakamaki, H., Miura, M., Aosaki, T., Masuda, M., Niwa, M., Kameyama, T., Kobayashi, J., Iwaki, Y., Imai, S., Ishikawa, A., Abe, K., Yoshimura, T., Nabeshima, T., and Ebihara, S. (2009) Usp46 is a quantitative trait gene regulating mouse immobile behavior in the tail suspension and forced swimming tests. *Nature Genetics*. **41**, 688–695

80. Kim, J. M., Parmar, K., Huang, M., Weinstock, D. M., Ruit, C. A., Kutok, J. L., and Andrea, A. D. D. (2009) Inactivation of Murine Usp1 Results in Genomic Instability and a Fanconi Anemia Phenotype. *Developmental Cell*. **16**, 314–320

81. Kon, N., Kobayashi, Y., Li, M., Brooks, C., Ludwig, T., and Gu, W. (2010) Inactivation of HAUSP in vivo modulates p53 function. *Oncogene*. **29**, 1270–1279

82. Rossi, A., Kontarakis, Z., Gerri, C., Nolte, H., Holper, S., Kruger, M., and Stainier, D. Y. R. (2015) Genetic compensation induced by deleterious mutations but not gene knockdowns. *Nature*. **524**, 230–233

83. Martin, L., Grigoryan, A., Wang, D., Wang, J., Breda, L., Cardozo, T., and Gardner, L. B. (2015) Identification and characterization of small molecules that inhibit nonsense mediated RNA decay and suppress nonsense p53 mutations. *Cancer Research*. **74**, 3104–3113

84. Isken, O., and Maquat, L. E. (2007) Quality control of eukaryotic mRNA : safeguarding cells from abnormal mRNA function. *Genes & Development*. **21**, 1833–1856